Published OnlineFirst February 23, 2011; DOI:10.1158/1078-0432.CCR-10-2008

promoter-driving *E1* gene-expressing shuttle plasmids having multiple tandem copies of sequences perfectly complementary to miRNAs in the 3′-UTR of the *E1* gene expression cassette were constructed as described below. A *Kpn*I/*Afl*III fragment of pHMCMV5 (22) was ligated with oligonucleotides miR-143T-S1 and miR-143T-AS1, which contain miR-143 complementary sequences, resulting in pHMCMV5-143T-1. The sequences of the oligonucleotides are shown in Supplementary Table S1. Next, a *Pac*I/*Afl*III fragment of pHMCMV5-143T-1 was ligated with oligonucleotides miR-143T-S2 and miR-143T-AS2. The resulting plasmid, pHMCMV5-143T, was digested with *I-Ceu*I after digestion with *Nhe*I followed by *Klenow* treatment, and then ligated with the *I-Ceu*I/*Pme*I fragment of pSh-hAIB (10), in which the *E1A* and *E1B* genes linked with an internal ribosomal entry site (IRES) are located downstream of the hTERT promoter, creating pSh-AIB-143T. For the construction of vector plasmids for TRADs, *I-Ceu*I/*PI-Sce*I-digested pSh-AIB-143T was ligated with the *I-Ceu*I/*PI-Sce*I-digested pAdHM3 (21), resulting in pAdHM3-AIB-143T. To generate TRADs, pAdHM3-AIB-143T was digested with *Pac*I and was transfected into 293 cells using Superfect transfection reagent (Qiagen). All TRADs were propagated in 293 cells, purified by 2 rounds of cesium chloride gradient ultracentrifugation, dialyzed, and stored at −80°C. TRADs containing other miRNA complementary sequences were similarly constructed using the corresponding oligonucleotides (Supplementary Table S1). The parental TRAD was similarly prepared using pSh-AIB and pAdHM3. The virus particles (VP) and biological titers were determined by a spectrophotometrical method (24) and by using an Adeno-X rapid titer kit (Clontech), respectively. The ratio of particle-to-biological titer was between 6 and 9 for each TRAD used in this study.

Determination of miRNA expression levels in human normal and tumor cells

Total RNA, including miRNAs, was isolated from cells using Isogen (Nippon Gene). After quantification of the RNA concentration, miRNA levels were determined using a TaqMan MiRNA reverse transcription kit, TaqMan miRNA assay kit, and ABI Prism 7000 system (Applied Biosystems). Amplification of U6 served as an endogenous control to normalize the miRNA expression data.

Infection with TRADs

Cells were seeded into 24-well plates at 5×10^4 cells/well. On the following day, cells were infected with TRADs at a multiplicity of infection (MOI) of 0.4 or 2 (for cancer cell lines), or of 10 (for normal cells), for 2 hours. Following incubation for 3 (for cancer cell lines) or 5 days (for normal cells), total DNA, including viral genomic DNA, was isolated from the cells using a DNeasy Blood & Tissue Kit (Qiagen). After isolation, the Ad genomic DNA contents were quantified using an ABI Prism 7000 system (Applied Biosystems) as previously described (25). The Ad genome copy numbers were normalized by the copy numbers of glyceroaldehyde-3-phosphate-dehydrogenase (GAPDH). Cell viability was also examined by crystal violet staining and Alamar blue assay at the indicated time points. To examine the miRNA-specific suppression of TRAD replication in normal human cells, 50 nmol/L of 2′-*O*-methylated antisense oligonucleotide complementary to miR-143 or miR-199a (Gene Design Inc.) was transfected into normal cells using Lipofectamine 2000 (Invitrogen). Twenty-four hours after transfection, the cells were infected with TRADs and replication of TRADs was evaluated as described above.

Real-time reverse transcriptase PCR analysis for *E1A* gene expression

Cells were seeded as described above and were infected with TRADs at an MOI of 2 (for cancer cells) or 10 (for normal cells) for 1.5 hours. After a 24 hour-incubation, total RNA was isolated, and reverse transcription reaction was carried out using a SuperScript II First-Strand Synthesis System (Invitrogen). E1A mRNA levels were determined with the E1A-specific primers and probe using an ABI prism 7000 system (26). The E1A mRNA levels were normalized by the GAPDH mRNA levels.

Statistical analysis

Statistical significance ($P < 0.05$) was determined using Student's t test. Data are presented as means ± SD.

Results

Replication of the conventional TRAD in normal human cells

First, to examine replication of the conventional TRAD in normal human cells, WI38 cells, which are human embryonic lung fibroblasts, were infected with the conventional TRAD at an MOI of 2 or 10 (Fig. 1). The conventional TRAD did not highly replicate in WI38 cells at an MOI of 2; however, an almost 500-fold increase in the Ad genome

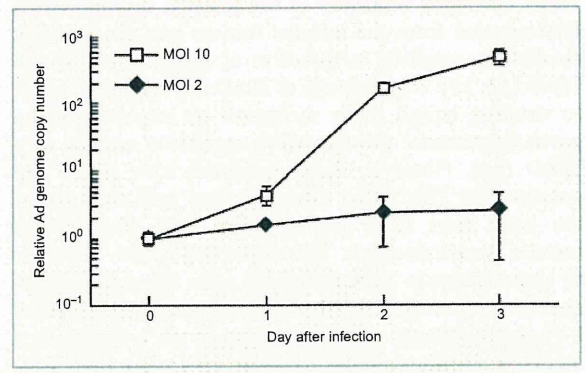

Figure 1. Replication of the conventional TRAD in WI38 cells. WI38 cells were infected with the conventional TRAD at an MOI of 2 or 10 for 2 hours. At the indicated time points, the copy numbers of the Ad genome and *GAPDH* gene were determined by real-time PCR. The ratio of the copy number of the Ad genome to that of GAPDH was normalized by the data on day 0. The data are shown as the means ± SD ($n = 3$).

Published OnlineFirst February 23, 2011; DOI:10.1158/1078-0432.CCR-10-2008

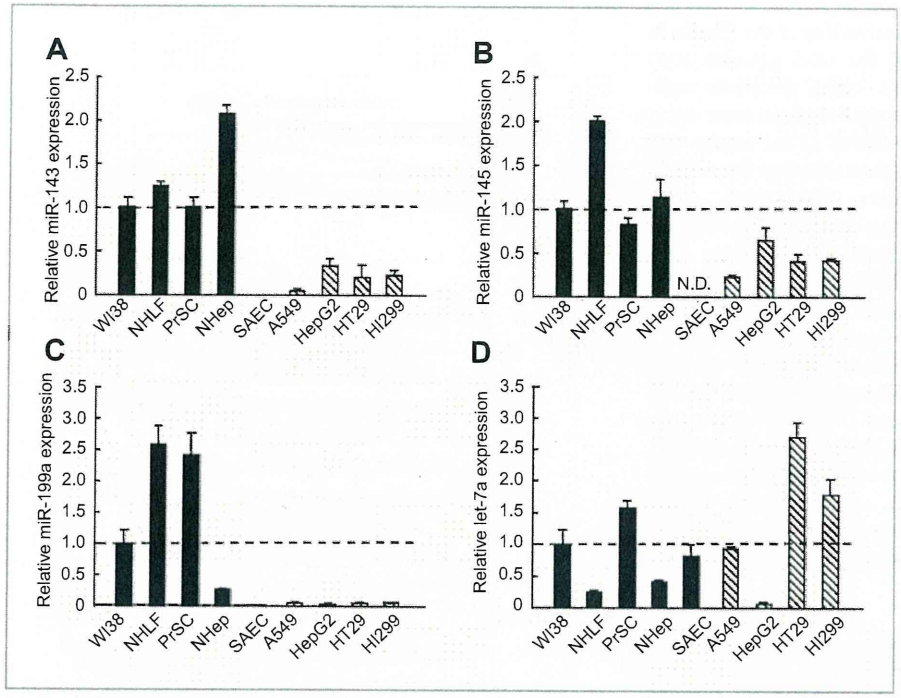

Figure 2. MiRNA expression levels in the human normal (solid bar) and tumor cells (hatched bar). MiRNA expression was determined by real-time RT-PCR. The ratio of miRNA to U6 expression levels was normalized by the data of WI38 cells. The data are shown as the means ± SD ($n = 3$). N.D., not detected.

was found 3 days after infection at an MOI of 10. These data indicate that the conventional TRAD replicates in normal human cells at a high MOI, even though tumor-specific hTERT promoters are used for the *E1* gene expression.

MiRNA expression levels in human tumor and normal cells

To examine the expression levels of miR-143, -145, -199a, and let-7a in the human normal and tumor cells, reverse transcriptase PCR (RT-PCR) analysis was carried out. Several studies have shown that these miRNAs are downregulated in various types of tumor cells isolated from cancer patients, compared with the corresponding normal tissues (16–18, 27). The expression levels of miR-143, -145, and -199a in the tumor cells were approximately 2- to 100-fold lower than those in the normal cells, although SAECs expression levels of miR-143, -145, and -199a were comparable or lower than those in the tumor cells (Fig. 2). In particular, a large reduction was found for miR-199a expression in all tumor cells, compared with the normal cells. On the other hand, the expression levels of let-7a in HT29 and H1299 cells were higher than those in the normal cells, although HepG2 cells expressed lower levels of let-7a than the normal cells. The absolute amounts of let-7a were more than 10-fold higher than those of the other miRNAs in all tumor and normal cells, except for NHLF, NHep, and HepG2 cells (data not shown).

Development of TRADs carrying an miRNA-regulated *E1* gene expression system

Next, to develop TRADs carrying a miRNA-regulated *E1* gene expression cassette (TRAD-miRT), we incorporated 4 copies of the perfectly complementary sequences for miR-143, -145, -199a, or let-7a into the 3′-UTR of the *E1* gene expression cassette (Fig. 3A). In TRADs, the *E1A* gene was connected with the *E1B* gene via IRES. We found that the expression of both the first and second gene in the IRES-containing expression cassette was suppressed in an miRNA-dependent manner by insertion of the miR-122a complementary sequences into the region downstream of the second gene in miR-122a-expressing Huh-7 cells, not in HepG2 cells, which express a low level of miR-122a (Supplementary Fig. S1), although it remains controversial whether miRNA-mediated posttranscriptional regulation can occur in an IRES-containing expression cassette (28–30). All TRADs were efficiently grown in normal 293 cells, and the ratios of infectious titers to physical titers were comparable among all the TRADs, including the parental TRAD.

Tumor cell lysis activity and replication of TRAD-miRT in tumor cells

To examine whether or not the inclusion of the sequences complementary to the miRNAs downregulated in tumor cells would inhibit the tumor cell lysis activity of TRADs, the viability of tumor cells was evaluated after infection with the TRADs. Almost all tumor cells were lysed by TRAD-143T, -145T, and -199aT at 3 days after infection, although cell lysis by TRAD-let7aT was largely inhibited (Fig. 3B). Furthermore, time-course studies of cell viability showed that TRAD-143T, -145T, and -199aT exhibited cytopathic efficacies comparable to that of the parental TRAD in the tumor cells at an MOI of 0.4 (Fig. 3C). Similar results were obtained at an MOI of 2 (data not shown).

Published OnlineFirst February 23, 2011; DOI:10.1158/1078-0432.CCR-10-2008

We next examined the replication ability of the TRADs in the tumor cells by determining the viral genome copy numbers. TRAD-143T, -145T, and -199aT efficiently replicated in the tumor cells, and the viral genome copy numbers of TRAD-143T, -145T, and -199aT in the tumor cells were more than 500-fold higher than those in the normal cells (data not shown). In addition, TRAD-143T, -145T, and -199aT exhibited viral genome copy numbers similar to that of the conventional TRAD in all tumor cells (Fig. 3D). All TRADs except for TRAD-let7aT also expressed similar levels of E1A mRNA (Fig. 3E). In contrast, insertion of let-7a complementary sequences largely inhibited the replication in all tumor cells. The E1A mRNA level was also reduced by 42% in H1299 cells infected with TRAD-let7aT. Inefficient replication of TRAD-let7aT in the tumor cells corresponded to the low cytopathic effects described above. These results indicate that TRADs containing the complementary sequences for miR-143, -145, or -199a exhibit efficient *E1* gene expression in the tumor cells and tumor cell lysis activity comparable to those of the conventional TRAD.

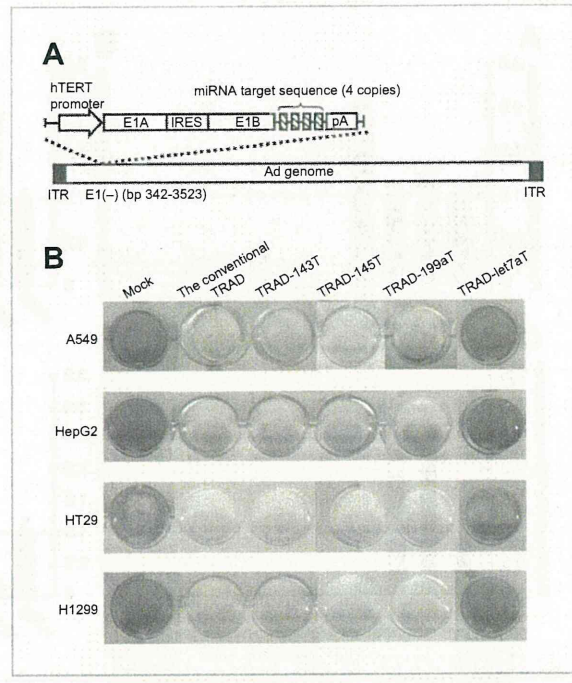

Figure 3. Replication and oncolytic activity of TRADs containing the miRNA complementary sequences in the tumor cells. A, a schematic diagram of a TRAD containing the miRNA-regulated *E1* gene expression system. ITR: inverted terminal repeat. B, crystal violet analysis of the cytopathic effects of TRADs in the tumor cells. The cells were infected with the TRADs at an MOI of 2 for 2 hours. Three days after infection, the cells were stained with crystal violet. The results are representative of at least 2 independent experiments. C, time-course study of the tumor cell lysis activity of TRADs by Alamar blue assay. The cells were infected with the TRADs at an MOI of 0.4 for 2 hours. At the indicated time points, the viability of the cells was analyzed by Alamar blue assay. The data were normalized by the data of the mock-infected group. D, the viral genome copy numbers of TRADs in the tumor cells. The cells were infected with the TRADs at an MOI of 2 for 2 hours. Three days after infection, the viral genome copy numbers were quantified by real-time PCR. The data was normalized by the data of the conventional TRAD group. E, the E1A mRNA levels in H1299 cells 24 hour after infection with the TRADs. The cells were infected with the TRADs at an MOI of 2 for 1.5 hours. Twenty-four hours after infection, the E1A mRNA levels were determined by real-time RT-PCR. The data was normalized by the data of the conventional TRAD group. All the data are shown as the means ± SD ($n = 3$–6). *, $P < 0.05$; **, $P < 0.005$.

Reduced replication of TRAD-miRT in normal cells

To examine whether replication of TRADs in normal cells is suppressed by incorporation of the sequences complementary to the miRNAs downregulated in tumor cells, normal human cells were infected with the TRADs. The virus genome copy numbers of TRAD-143T, -145T, and -199aT were 5- to 1,000-fold reduced, compared with the conventional TRAD at 5 days following infection in WI38 cells (Fig. 4A). An approximately 3- to 300-fold reduction in the genome copy numbers of TRAD-143T, -145T, and -199aT was also observed in NHLF and PrSC. The replication of TRADs was also suppressed in SAEC by the insertion of the miRNA complementary sequences, although the expression levels of miR-143, -145, and -199a in SAEC were much lower than those in the other normal cells (Fig. 2). The suppressive effects of insertion of the miRNA target sequences were different among the cells; however, overall, the insertion of miR-199a complementary sequences mediated similar or higher suppressive effects on the replication of TRADs in all the normal cells examined, compared with insertion of the sequences complementary to miR-143 and -145. Replication of TRAD-199aT was inhibited by more than 10-fold in all the normal cells except for SAEC. We also examined the viabilities of the normal cells after infection with the TRADs. No apparent differences in cell viabilities were found among the TRADs by crystal violet staining (data not shown); however, Alamar blue assay showed that the average values of the normal cell viabilities were higher after infection with TRAD-miRT than after infection with the conventional TRAD (Fig. 4B). These results suggest that the suppression of TRAD replication by insertion of the miRNA complementary sequences results in the improvement of the TRAD safety profile in normal cells.

Next, to evaluate whether the reduction in replication of TRAD-miRT was miRNA-dependent, miRNAs were inhibited by a 2′-*O*-methylated antisense oligonucleotide. NHLF and PrSC cells were transfected with the 2′-*O*-methylated antisense oligonucleotide against miR-143 or -199a, and then the cells were infected with the TRADs, 24 hour after transfection. In the cells transfected with the 2′-*O*-methylated antisense oligonucleotide against miR-143 or -199a, the reduction in the replication of TRAD-miRT was significantly restored, but the scramble 2′-*O*-methylated oligonucleotide did not significantly affect the replication of TRAD-miRT (Fig. 4C). These results indicate that the reduction in the replication of TRAD-miRT in the normal cells was miRNA-dependent.

Published OnlineFirst February 23, 2011; DOI:10.1158/1078-0432.CCR-10-2008

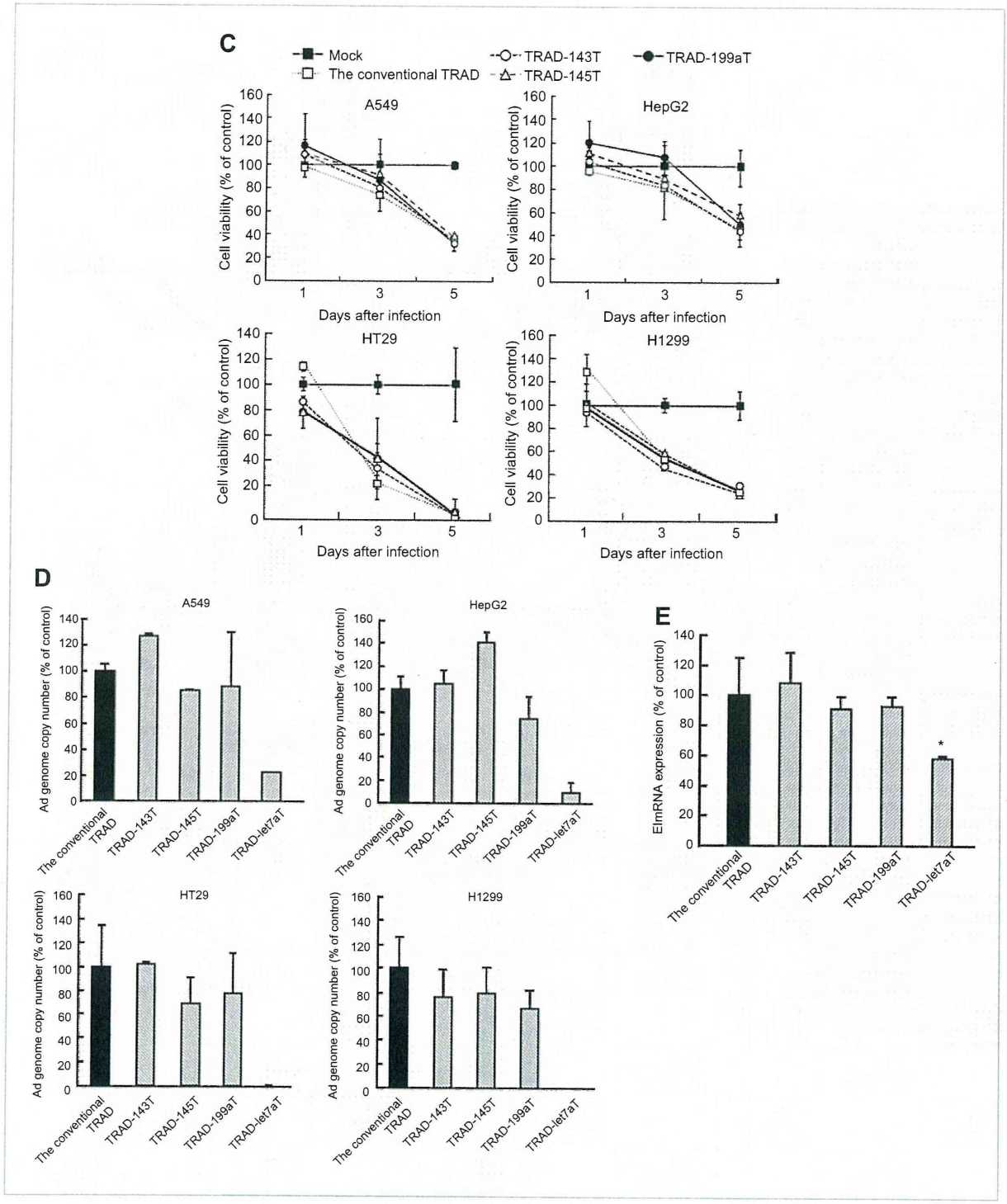

Figure 3. (*Continued*)

Published OnlineFirst February 23, 2011; DOI:10.1158/1078-0432.CCR-10-2008

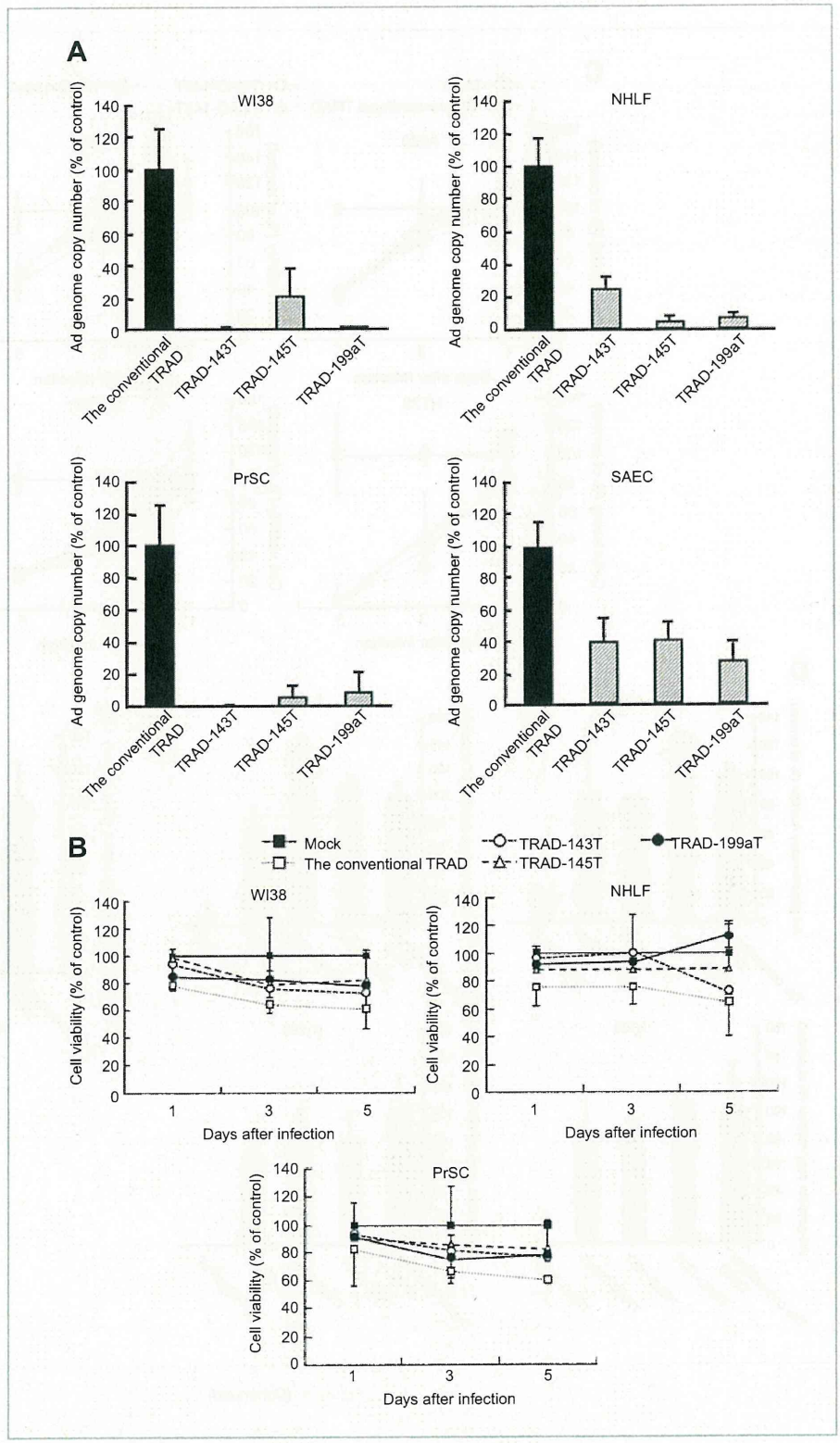

Figure 4. Reduced replication of TRADs in normal human cells by insertion of the miRNA complementary sequences. A, the viral genome copy numbers of TRADs in normal cells. The cells were infected with the TRADs at an MOI of 10 for 2 hours. Five days after infection, the viral genome copy numbers were determined by real-time PCR. B, time-course study of the normal human cell viabilities after infection with TRADs by Alamar blue assay. The cells were infected with the TRADs at an MOI of 10 for 2 hours. At the indicated time points, the viability of the cells was analyzed by Alamar blue assay. The data were normalized by the data of the mock-infected group. C, restoration of TRAD replication in human normal cells by 2′-*O*-methylated antisense oligonucleotides. The cells were transfected with 50 nmol/L of 2′-*O*-methylated antisense oligonucleotides for miR-143 or -199a. Twenty-four hours after transfection, the cells were infected with the TRADs at an MOI of 10, and the viral genome copy numbers were determined 5 days after infection with the TRADs. D, the E1A mRNA levels in normal human cells. The cells were infected with the TRADs at an MOI of 10 for 1.5 hours. Twenty-four hours after infection, the E1 mRNA levels were determined by real-time RT-PCR. The data was normalized by the data of the conventional TRAD group. All the data are shown as the means ± SD ($n = 3$–4). *, $P < 0.05$; **, $P < 0.005$.

Published OnlineFirst February 23, 2011; DOI:10.1158/1078-0432.CCR-10-2008

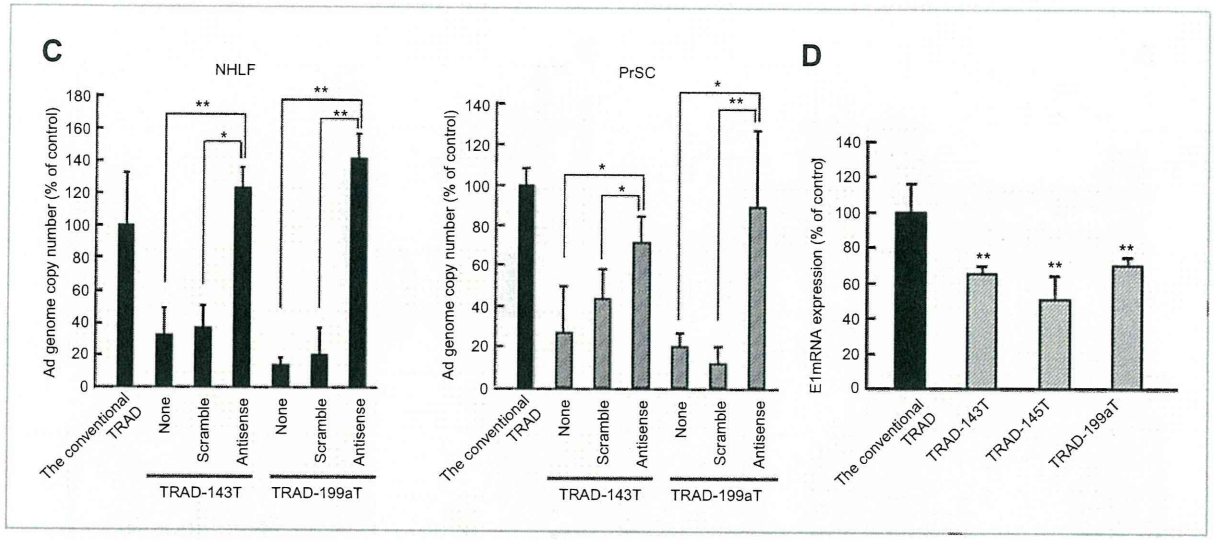

Figure 4. (*Continued*)

E1A expression by TRAD-miRT in normal cells

To determine whether incorporation of the miRNA complementary sequences into the *E1* gene expression cassette decreases the *E1* mRNA levels in normal human cells, real-time RT-PCR analysis for the E1A mRNA levels wascarried out. The E1A mRNA levels were reduced by more than 30% for TRAD-143T, -145T, and -199aT, compared with the parent TRAD, in NHLF (Fig. 4D). The reduction in the E1A mRNA levels corresponded to the suppression in replication of TRAD-miRT, indicating that miRNA-mediated reduction in the *E1* gene expression resulted in a reduced replication of TRAD-miRT.

Development of TRADs containing the complementary sequences for liver-specific miRNA

To prevent the replication of TRADs in liver hepatocytes as well as other normal cells, we incorporated not only miR-199a complementary sequences but also sequences complementary to liver-specific miR-122a into the *E1* gene expression cassette, resulting in TRAD-122a/199aT (Fig. 5A). It is well known that Ads have high hepatic tropism, leading to efficient liver accumulation even after local administration. MiR-122a was expressed approximately 100- and 20-fold more abundantly in NHep and Huh-7 cells, respectively, than in the other normal human cells and tumor cells (Fig. 5B); conversely, the other normal cells expressed more than 10-fold lower levels of miR-122a than miR-143, -145, and -199a (data not shown). Incorporation of miR-122a complementary sequences alone significantly reduced the virus genome copy number of TRAD-122aT in NHLF and NHep; however, no statistically significant decrease in the genome copy number of TRAD-122aT was found in PrSC (Fig. 5C). On the other hand, insertion of miR-199a target sequences alone was less efficient than insertion of miR-122a target sequences in NHep, probably due to the lower expression of miR-199a than miR-122a in NHep. By contrast, insertion of both miR-122a and miR-199a target sequences into the *E1* gene expression cassette efficiently reduced the replication of TRAD-122a/199aT by 10- to 50-fold in all normal cells examined. Significantly reduced replication of TRAD-122a and TRAD-122a/199aT was also found in Huh-7 cells, which are a hepatoma cell line highly expressing miR-122a and are often used as a model of hepatocytes (Supplementary Fig. S2). The incorporation of the miR-145 complementary sequences was also effective for suppressing the TRAD replication in NHep (Supplementary Fig. S3). The E1A mRNA levels were reduced for TRAD-122aT and -122a/199aT in NHep (Fig. 5D). In addition, TRAD-122a/199aT efficiently replicated in the tumor cells, resulting in efficient tumor cell lysis (Fig. 5E and F). These results indicate that replication of the TRADs in various types of normal human cells, including liver hepatocytes, is significantly reduced by insertion of the multiple target sequences to both miR-122a and -199a, without influencing the tumor cell lysis activity.

Discussion

The aim of this study was to prevent the replication of TRADs in normal human cells by incorporation of sequences complementary to miRNAs that are selectively downregulated in tumor cells, without altering the tumor cell lysis activity. Currently, there is no appropriate animal model which fully supports the *in vivo* replication of Ads and evaluation of the *in vivo* toxicity caused by oncolytic Ads, and thus it is important to be cautious in regard to oncolytic Ad-induced toxicity. To prevent the *E1* gene expression and replication of oncolytic Ads in normal cells as much as possible, an miRNA-mediated posttranscriptional detargeting system was included in TRADs, in

Published OnlineFirst February 23, 2011; DOI:10.1158/1078-0432.CCR-10-2008

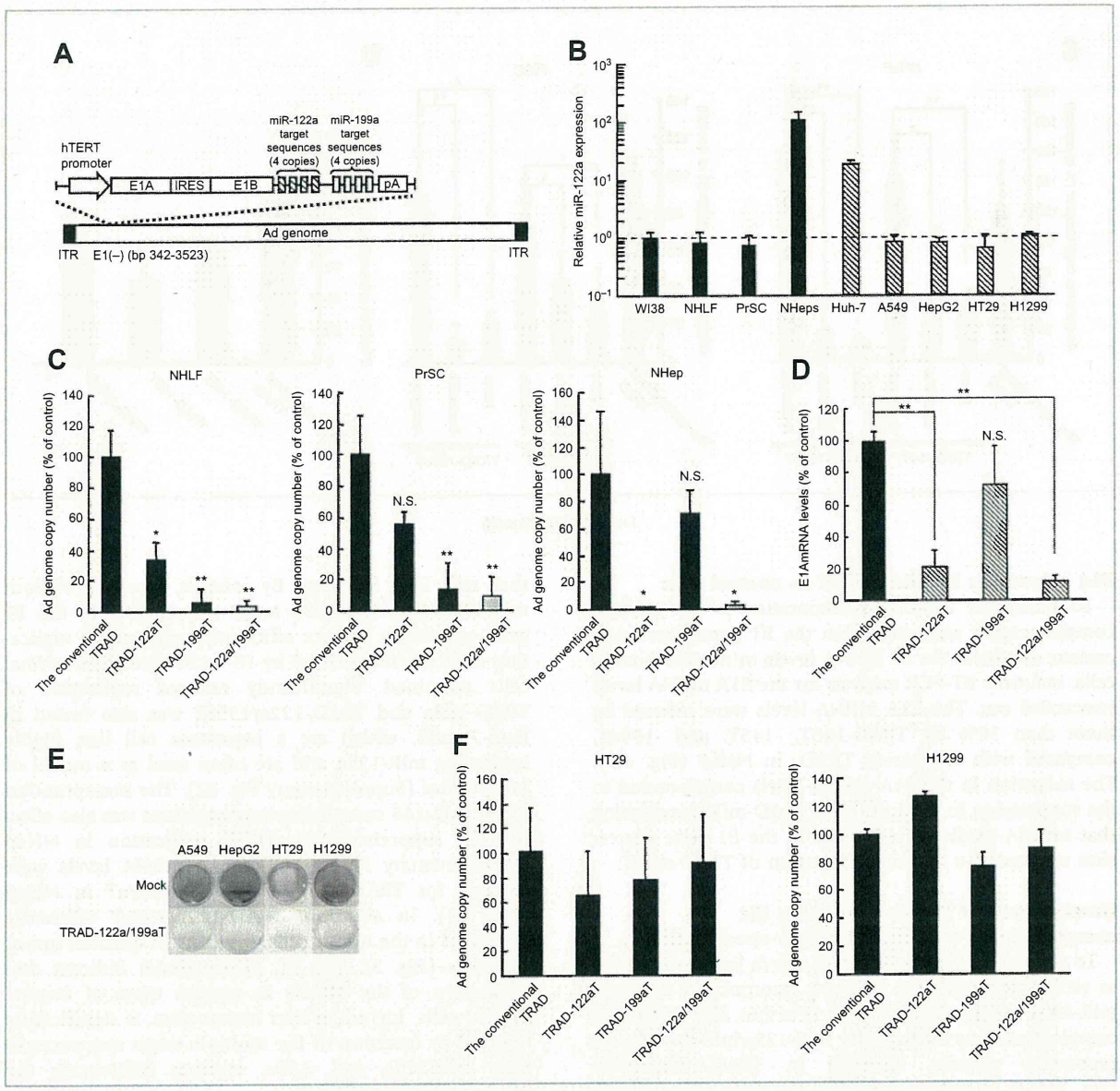

Figure 5. Tumor cell lysis activity and enhanced safety profile of TRAD-122a/199aT. A, a schematic diagram of TRAD-122a/199aT. B, miR-122a expression levels in the normal and tumor cells. C, the viral genome copy numbers of TRAD-122a/199aT in normal human cells. D, the E1A mRNA levels in NHep. E, crystal violet analysis for the cytopathic effects of TRAD-122a/199aT. The results are representative of 2 independent experiments. F, the viral genome copy numbers of TRAD-122a/199aT in tumor cells. The tumor and normal cells were infected with the TRADs at an MOI of 2 (tumor cells) or 10 (normal cells) for 2 hours. The cells were stained with crystal violet 3 days after infection. The viral genome copy numbers were determined 3 (tumor cells) or 5 days (normal cells) after infection. For determination of the E1A mRNA levels, total RNA was isolated from NHep 24 hour after infection with the TRADs at an MOI of 10, and the E1A mRNA levels were determined by real-time RT-PCR. The data was normalized by the data of the conventional TRAD group. All the data are shown as the means ± SD (n = 3–6). N.S.: not significantly different. *, $P < 0.05$; **, $P < 0.005$.

addition to the transcriptional targeting system via tumor-specific promoters.

As described above, TRAD replicates in the injected tumors and is disseminated from the injected tumors into the systemic circulation, leading to infection of distant, uninjected tumors (11, 13, 14). This property of TRAD had led to a concern that TRAD could infect normal cells over the whole body, including the hepatocytes, after dissemination from the injected tumors. It is crucial that such unexpected infection of normal cells by TRAD is prevented. Previous studies have shown that insertion of sequences complementary to liver-specific miR-122a reduced the replication of oncolytic Ads in Huh-7 cells, which are a model cell for hepatocytes (31–33). It is especially crucial

Published OnlineFirst February 23, 2011; DOI:10.1158/1078-0432.CCR-10-2008

to prevent the replication of TRAD in the liver, because Ad vectors have strong hepatotropism. However, TRAD also might infect normal cells other than hepatocytes, indicating that replication of oncolytic Ads in normal cells other than hepatocytes should also be suppressed. To prevent the replication of TRADs in other normal cells, we incorporated the sequences complementary to miR-143, -145, -199a, or let-7a, which are downregulated in the tumors and widely expressed in normal cells. The expression levels of these miRNAs in the tumor cells were lower than those in the normal cells in this study, and insertion of sequences complementary to miR-143, -145, or -199a significantly reduced the E1A mRNA levels and the replication of TRADs in the normal cells.

Overall, among the miRNA complementary sequences, the miR-199a complementary sequences appeared to be the most efficient at suppressing the replication of TRADs across all the normal cells except for hepatocytes; however, insertion of miR-199a target sequences alone failed to significantly reduce the replication of TRADs in the hepatocytes. To simultaneously prevent the replication of TRADs in various types of normal cells, including hepatocytes, we incorporated sequences complementary to miR-122a, which is abundantly expressed in hepatocytes, in addition to miR-199a target sequences. Brown and colleagues reported that a desired transgene expression pattern was achieved, depending on the miRNA expression profile, by incorporation of target sequences for 2 distinct miRNAs (34). TRAD-122aT/199aT exhibited more than 10-fold reduction in the replication in all the normal cells except for SAEC, although insertion of target sequences for miR-122a or miR-199a alone failed to suppress the replication of TRADs in either of the normal cells. Furthermore, TRAD-122aT/199aT and the parental TRAD mediated similar cytopathic efficacies in the tumor cells. These results indicate that replication of TRADs in not only hepatocytes but also other normal cells is simultaneously reduced by insertion of both miR-122a complementary sequences and sequences complementary to miRNAs highly expressed in normal cells, without altering the tumor cell lysis activity.

TRADs containing miR-122a complementary sequences are also considered to be promising for the treatment of liver cancer because miR-122a is significantly downregulated in liver cancer cells (35–37) leading to efficient replication and lytic activity of TRADs containing miR-122a complementary sequences in liver cancer cells. This study has shown that TRAD-122aT/199aT caused efficient cell lysis in a hepatocellular carcinoma cell line, HepG2 cells, while the replication of TRADs containing the miR-122a complementary sequences in normal hepatocytes, which highly express miR-122a, was significantly inhibited.

The expression levels of miRNAs are a crucial factor to suppress the gene expression by miRNAs. Brown and colleagues showed that miRNAs should be expressed at a concentration above the threshold (>100 copies/pg small RNA) to induce miRNA-regulated suppression of transgene expression (34). We were not able to precisely show the expression levels of miRNAs as the ratio of copies/pg small RNA in this study; however, comparing the miRNA levels in this study with those reported by Brown and colleagues (34), we consider that the expression levels of miR-143, -145, and -199a in the normal cells were higher than 100 copies/pg small RNA, leading to efficient suppression of the replication of TRADs.

Several studies have shown that let-7, including let-7a, is significantly downregulated in tumor cells (16, 19, 20). Edge and colleagues reported that insertion of let-7a complementary sequences into the matrix protein expression cassette of the vesicular somatitis virus (VSV) suppressed the replication of VSV in human primary fibroblast MG38 cells; on the other hand, VSV carrying let-7a target sequences efficiently replicated in A549 cells (38). However, our data showed that cancer cell lines other than HepG2 cells expressed similar or higher levels of let-7a than the normal cells. In addition, the expression levels of let-7a were more than 10-fold higher than those of the other miRNAs in the tumor cells. Abundant let-7a expression leads to a reduction in the replication of TRAD-let7aT in tumor cells. Furthermore, the members of the let-7 family, including let-7b and let-7c, have the same seed sequence, suggesting that let-7 family members other than let-7a would also contribute to the significant suppression of replication of TRAD-let7aT. These results suggest that not only expression profiles of miRNAs but also absolute amounts of miRNA expression in the cells are of great importance for miRNA-regulated gene expression.

Our data showed that the E1A mRNA levels were reduced by approximately 30% to 50% for TRAD-143T, -145T, and -199aT, compared with the conventional TRAD 24 hour after infection with the normal cells. These reduction levels in the E1A mRNA were much smaller than those in the Ad genome copy numbers at 5 days after infection; however, these reductions in the E1A mRNA levels would lead to large differences in the Ad genome copy numbers after several virus replication cycles. More than 5-fold reductions in the E1A mRNA were found for TRAD-143T, -145T, and -199aT, compared with the parental TRAD, 5 days after infection with the normal cells (data not shown).

A phase I clinical trial of the parental TRAD was conducted, and serious adverse events were not observed (3). In this study, efficient replication of the conventional TRAD in WI38 cells was found at an MOI of 10; however, the conventional TRAD did not exhibit a high level of replication at an MOI of 2. It might be unlikely that such a high titer (MOI 10) of oncolytic Ad would infect organs distal from the injection points in clinical trials; however, normal cells around the injection points might be infected with a high titer of oncolytic Ad. In addition, even though no apparent replication of TRADs is observed in normal cells after infection of TRADs, the expression of Ad proteins, including E1A and E4 proteins, affects the cellular functions via various mechanisms (39–41). This study indicates that inclusion of an miRNA-regulated *E1* gene expression system in oncolytic Ads enhances the safety of oncolytic Ads and makes it possible to increase the injection doses, leading to superior therapeutic effects.

Published OnlineFirst February 23, 2011; DOI:10.1158/1078-0432.CCR-10-2008

In summary, we developed TRADs in which the *E1* gene expression is controlled by miRNAs more highly expressed in normal cells than tumor cells. The TRADs containing the sequences complementary to miR-143, -145, or -199a exhibited reduced replication in the normal cells without altering the tumor cell lysis activity. Furthermore, incorporation of both miR-199a and miR-122a target sequences significantly suppressed the replication in all human primary cells examined, including hepatocytes. TRAD-miRT has enhanced both the safety profiles and comparable tumor cell lysis activity to the parental TRAD, suggesting that TRAD-miRT offers great potential for the treatment of tumors.

Disclosure of Potential Conflicts of Interest

Toshiyoshi Fujiwara and Hiroyuki Mizuguchi are consultants to Oncolys BioPharma, Inc. No other potential conflicts of interest were disclosed.

References

1. Mathis JM, Stoff-Khalili MA, Curiel DT. Oncolytic adenoviruses—selective retargeting to tumor cells. Oncogene 2005;24:7775–91.
2. Ribacka C, Pesonen S, Hemminki A. Cancer, stem cells, and oncolytic viruses. Ann Med 2008;40:496–505.
3. Nemunaitis J, Tong AW, Nemunaitis M, Senzer N, Phadke AP, Bedell C, et al. A phase I study of telomerase-specific replication competent oncolytic adenovirus (telomelysin) for various solid tumors. Mol Ther 2010;18:429–34.
4. Li JL, Liu HL, Zhang XR, Xu JP, Hu WK, Liang M, et al. A phase I trial of intratumoral administration of recombinant oncolytic adenovirus overexpressing HSP70 in advanced solid tumor patients. Gene Ther 2009;16:376–82.
5. Freytag SO, Movsas B, Aref I, Stricker H, Peabody J, Pegg J, et al. Phase I trial of replication-competent adenovirus-mediated suicide gene therapy combined with IMRT for prostate cancer. Mol Ther 2007;15:1016–23.
6. Li Y, Yu DC, Chen Y, Amin P, Zhang H, Nguyen N, et al. A hepatocellular carcinoma-specific adenovirus variant, CV890, eliminates distant human liver tumors in combination with doxorubicin. Cancer Res 2001;61:6428–36.
7. Rodriguez R, Schuur ER, Lim HY, Henderson GA, Simons JW, Henderson DR. Prostate attenuated replication competent adenovirus (ARCA) CN706: a selective cytotoxic for prostate-specific antigen-positive prostate cancer cells. Cancer Res 1997;57:2559–63.
8. Matsubara S, Wada Y, Gardner TA, Egawa M, Park MS, Hsieh CL, et al. A conditional replication-competent adenoviral vector, Ad-OC-E1a, to cotarget prostate cancer and bone stroma in an experimental model of androgen-independent prostate cancer bone metastasis. Cancer Res 2001;61:6012–9.
9. Yamamoto M, Davydova J, Wang M, Siegal GP, Krasnykh V, Vickers SM, et al. Infectivity enhanced, cyclooxygenase-2 promoter-based conditionally replicative adenovirus for pancreatic cancer. Gastroenterology 2003;125:1203–18.
10. Kawashima T, Kagawa S, Kobayashi N, Shirakiya Y, Umeoka T, Teraishi F, et al. Telomerase-specific replication-selective virotherapy for human cancer. Clin Cancer Res 2004;10:285–92.
11. Taki M, Kagawa S, Nishizaki M, Mizuguchi H, Hayakawa T, Kyo S, et al. Enhanced oncolysis by a tropism-modified telomerase-specific replication-selective adenoviral agent OBP-405 ('Telomelysin-RGD'). Oncogene 2005;24:3130–40.
12. Watanabe T, Hioki M, Fujiwara T, Nishizaki M, Kagawa S, Taki M, et al. Histone deacetylase inhibitor FR901228 enhances the antitumor effect of telomerase-specific replication-selective adenoviral agent OBP-301 in human lung cancer cells. Exp Cell Res 2006;312:256–65.
13. Umeoka T, Kawashima T, Kagawa S, Teraishi F, Taki M, Nishizaki M, et al. Visualization of intrathoracically disseminated solid tumors in mice with optical imaging by telomerase-specific amplification of a transferred green fluorescent protein gene. Cancer Res 2004;64:6259–65.
14. Kishimoto H, Kojima T, Watanabe Y, Kagawa S, Fujiwara T, Uno F, et al. In vivo imaging of lymph node metastasis with telomerase-specific replication-selective adenovirus. Nat Med 2006;12:1213–9.
15. Hitt MM, Graham FL. Adenovirus E1A under the control of heterologous promoters: wide variation in E1A expression levels has little effect on virus replication. Virology 1990;179:667–78.
16. Takamizawa J, Konishi H, Yanagisawa K, Tomida S, Osada H, Endoh H, et al. Reduced expression of the let-7 microRNAs in human lung cancers in association with shortened postoperative survival. Cancer Res 2004;64:3753–6.
17. Michael MZ, SM OC, van Holst Pellekaan NG, Young GP, James RJ. Reduced accumulation of specific microRNAs in colorectal neoplasia. Mol Cancer Res 2003;1:882–91.
18. Slaby O, Svoboda M, Fabian P, Smerdova T, Knoflickova D, Bednarikova M, et al. Altered expression of miR-21, miR-31, miR-143 and miR-145 is related to clinicopathologic features of colorectal cancer. Oncology 2007;72:397–402.
19. Yanaihara N, Caplen N, Bowman E, Seike M, Kumamoto K, Yi M, et al. Unique microRNA molecular profiles in lung cancer diagnosis and prognosis. Cancer Cell 2006;9:189–98.
20. Johnson SM, Grosshans H, Shingara J, Byrom M, Jarvis R, Cheng A, et al. RAS is regulated by the let-7 microRNA family. Cell 2005;120:635–47.
21. Mizuguchi H, Kay MA. Efficient construction of a recombinant adenovirus vector by an improved in vitro ligation method. Hum Gene Ther 1998;9:2577–83.
22. Mizuguchi H, Kay MA. A simple method for constructing E1- and E1/E4-deleted recombinant adenoviral vectors. Hum Gene Ther 1999;10:2013–7.
23. Sakurai F, Kawabata K, Yamaguchi T, Hayakawa T, Mizuguchi H. Optimization of adenovirus serotype 35 vectors for efficient transduction in human hematopoietic progenitors: comparison of promoter activities. Gene Ther 2005;12:1424–33.
24. Maizel JV Jr, White DO, Scharff MD. The polypeptides of adenovirus. I. Evidence for multiple protein components in the virion and a comparison of types 2, 7A, and 12. Virology 1968;36:115–25.
25. Koizumi N, Kawabata K, Sakurai F, Watanabe Y, Hayakawa T, Mizuguchi H. Modified adenoviral vectors ablated for coxsackievirus-adenovirus receptor, alphav integrin, and heparan sulfate binding reduce in vivo tissue transduction and toxicity. Hum Gene Ther 2006;17:264–79.
26. Ishii-Watabe A, Uchida E, Iwata A, Nagata R, Satoh K, Fan K, et al. Detection of replication-competent adenoviruses spiked into recombinant adenovirus vector products by infectivity PCR. Mol Ther 2003;8:1009–16.

Acknowledgments

We thank Takako Ichinose, Koyori Yano (National Institute of Biomedical Innovation, Osaka, Japan), and Sayuri Okamoto (Graduate School of Pharmaceutical Sciences, Osaka University, Osaka, Japan) for their help.

Grant Support

Support was received from a grant-in-aid for Young Scientists (A) F. Sakurai from the Ministry of Education, Culture, Sports, Science, and Technology (MEXT) of Japan (F. Sakurai), and a grant from the Takeda Science Foundation (H. Mizuguchi).

The costs of publication of this article were defrayed in part by the payment of page charges. This article must therefore be hereby marked *advertisement* in accordance with 18 U.S.C. Section 1734 solely to indicate this fact.

Received July 28, 2010; revised November 18, 2010; accepted December 14, 2010; published OnlineFirst February 23, 2011.

Published OnlineFirst February 23, 2011; DOI:10.1158/1078-0432.CCR-10-2008

27. Iorio MV, Visone R, Di Leva G, Donati V, Petrocca F, Casalini P, et al. MicroRNA signatures in human ovarian cancer. Cancer Res 2007;67:8699–707.
28. Mathonnet G, Fabian MR, Svitkin YV, Parsyan A, Huck L, Murata T, et al. MicroRNA inhibition of translation initiation in vitro by targeting the cap-binding complex eIF4F. Science 2007;317:1764–7.
29. Petersen CP, Bordeleau ME, Pelletier J, Sharp PA. Short RNAs repress translation after initiation in mammalian cells. Mol Cell 2006;21:533–42.
30. Pillai RS, Bhattacharyya SN, Artus CG, Zoller T, Cougot N, Basyuk E, et al. Inhibition of translational initiation by Let-7 MicroRNA in human cells. Science 2005;309:1573–6.
31. Cawood R, Chen HH, Carroll F, Bazan-Peregrino M, van Rooijen N, Seymour LW. Use of tissue-specific microRNA to control pathology of wild-type adenovirus without attenuation of its ability to kill cancer cells. PLoS Pathog 2009;5:e1000440.
32. Leja J, Nilsson B, Yu D, Gustafson E, Akerstrom G, Oberg K, et al. Double-detargeted oncolytic adenovirus shows replication arrest in liver cells and retains neuroendocrine cell killing ability. PLoS One 2010;5:e8916.
33. Ylosmaki E, Hakkarainen T, Hemminki A, Visakorpi T, Andino R, Saksela K. Generation of a conditionally replicating adenovirus based on targeted destruction of E1A mRNA by a cell type-specific MicroRNA. J Virol 2008;82:11009–15.
34. Brown BD, Gentner B, Cantore A, Colleoni S, Amendola M, Zingale A, et al. Endogenous microRNA can be broadly exploited to regulate transgene expression according to tissue, lineage and differentiation state. Nat Biotechnol 2007;25:1457–67.
35. Coulouarn C, Factor VM, Andersen JB, Durkin ME, Thorgeirsson SS. Loss of miR-122 expression in liver cancer correlates with suppression of the hepatic phenotype and gain of metastatic properties. Oncogene 2009;28:3526–36.
36. Bai S, Nasser MW, Wang B, Hsu SH, Datta J, Kutay H, et al. MicroRNA-122 inhibits tumorigenic properties of hepatocellular carcinoma cells and sensitizes these cells to sorafenib. J Biol Chem 2009;284:32015–27.
37. Gramantieri L, Ferracin M, Fornari F, Veronese A, Sabbioni S, Liu CG, et al. Cyclin G1 is a target of miR-122a, a microRNA frequently downregulated in human hepatocellular carcinoma. Cancer Res 2007;67:6092–9.
38. Edge RE, Falls TJ, Brown CW, Lichty BD, Atkins H, Bell JC. A let-7 MicroRNA-sensitive vesicular stomatitis virus demonstrates tumor-specific replication. Mol Ther 2008;16:1437–43.
39. Duerksen-Hughes P, Wold WS, Gooding LR. Adenovirus E1A renders infected cells sensitive to cytolysis by tumor necrosis factor. J Immunol 1989;143:4193–200.
40. Ramalingam R, Worgall S, Rafii S, Crystal RG. Downregulation of CXCR4 gene expression in primary human endothelial cells following infection with E1(-)E4(+) adenovirus gene transfer vectors. Mol Ther 2000;2:381–6.
41. Weitzman MD. Functions of the adenovirus E4 proteins and their impact on viral vectors. Front Biosci 2005;10:1106–17.

MTOpen

Efficient Generation of Hepatoblasts From Human ES Cells and iPS Cells by Transient Overexpression of Homeobox Gene *HEX*

Mitsuru Inamura[1,2], Kenji Kawabata[2,3], Kazuo Takayama[1,2], Katsuhisa Tashiro[2], Fuminori Sakurai[2], Kazufumi Katayama[1,2], Masashi Toyoda[4], Hidenori Akutsu[4], Yoshitaka Miyagawa[5], Hajime Okita[5], Nobutaka Kiyokawa[5], Akihiro Umezawa[4], Takao Hayakawa[6,7], Miho K Furue[8,9] and Hiroyuki Mizuguchi[1,2]

[1]*Department of Biochemistry and Molecular Biology, Graduate School of Pharmaceutical Sciences, Osaka University, Osaka, Japan;* [2]*Laboratory of Stem Cell Regulation, National Institute of Biomedical Innovation, Osaka, Japan;* [3]*Department of Biomedical Innovation, Graduate School of Pharmaceutical Science, Osaka University, Osaka, Japan;* [4]*Department of Reproductive Biology, National Institute for Child Health and Development, Tokyo, Japan;* [5]*Department of Developmental Biology and Pathology, National Institute for Child Health and Development, Tokyo, Japan;* [6]*Pharmaceutics and Medical Devices Agency, Tokyo, Japan;* [7]*Pharmaceutical Research and Technology Institute, Kinki University, Osaka, Japan;* [8]*JCRB Cell Bank/Laboratory of Cell Culture, Department of Disease Bioresource, National Institute of Biomedical Innovation, Osaka, Japan;* [9]*Laboratory of Cell Processing, Institute for Frontier Medical Sciences, Kyoto University, Kyoto, Japan*

Human embryonic stem cells (ESCs) and induced pluripotent stem cells (iPSCs) have the potential to differentiate into all cell lineages, including hepatocytes, *in vitro*. Induced hepatocytes have a wide range of potential application in biomedical research, drug discovery, and the treatment of liver disease. However, the existing protocols for hepatic differentiation of PSCs are not very efficient. In this study, we developed an efficient method to induce hepatoblasts, which are progenitors of hepatocytes, from human ESCs and iPSCs by overexpression of the *HEX* gene, which is a homeotic gene and also essential for hepatic differentiation, using a HEX-expressing adenovirus (Ad) vector under serum/feeder cell-free chemically defined conditions. Ad-HEX-transduced cells expressed α-fetoprotein (AFP) at day 9 and then expressed albumin (ALB) at day 12. Furthermore, the Ad-HEX-transduced cells derived from human iPSCs also produced several cytochrome P450 (CYP) isozymes, and these P450 isozymes were capable of converting the substrates to metabolites and responding to the chemical stimulation. Our differentiation protocol using Ad vector-mediated transient HEX transduction under chemically defined conditions efficiently generates hepatoblasts from human ESCs and iPSCs. Thus, our methods would be useful for not only drug screening but also therapeutic applications.

Received 18 March 2010; accepted 13 October 2010; published online 23 November 2010. doi:10.1038/mt.2010.241

INTRODUCTION

Human embryonic stem cells (ESCs) and induced pluripotent stem cells (iPSCs) are able to replicate indefinitely and differentiate into most cell types of the body,[1–4] and thereby have the potential to provide an unlimited source of cells for a variety of applications.[5] Hepatocytes are useful cells for biomedical research, regenerative medicine, and drug discovery. They are particularly applicable to drug screenings, such as for the determination of metabolic and toxicological properties of drug compounds in *in vitro* models, because the liver is the main detoxification organ in the body.[6] For these applications, it is necessary to prepare a large number of functional hepatocytes from human ESCs and iPSCs. Many of the existing methods for cell differentiation of human ESCs and iPSCs into hepatocytes employ undefined, serum-containing medium and feeder cells.[7–9] Preparation of human ESC- and iPSC-derived hepatocytes for therapeutic applications and drug toxicity testing in humans should be done in nonxenogenic culture systems to avoid potential contamination with pathogens. Furthermore, the efficiency of the differentiation of the human ESCs and iPSCs into hepatocytes is not particularly high using these methods.[9–14]

In vertebrate development, the liver is derived from the primitive gut tube, which is formed by a flat sheet of cells called the definitive endoderm.[5,15] Shortly afterwards, the definitive endoderm is separated into endoderm derivatives containing the liver bud, the cells of which are referred to as hepatoblasts. The hepatoblasts have the potential to proliferate and differentiate into both hepatocytes and cholangiocytes. In the process of hepatic differentiation, the maturation is characterized by the expression of liver- and stage-specific genes. For example, α-fetoprotein (AFP) is an early hepatic marker, which is expressed in hepatoblasts in the liver bud until birth, and its expression is dramatically reduced after birth.[16] In contrast, albumin (ALB), which is the most abundant protein synthesized by hepatocytes, is initially expressed at lower levels in early fetal hepatocytes, but its expression level is increased as the hepatocytes mature, reaching a maximum in adult hepatocytes.[17] Furthermore, isoforms of cytochrome P450 (CYP) proteins also exhibit differential expression levels according to the developmental stages

Correspondence: *Hiroyuki Mizuguchi, Department of Biochemistry and Molecular Biology, Graduate School of Pharmaceutical Sciences, Osaka University, 1-6 Yamadaoka, Suita, Osaka 565-0871, Japan. E-mail: mizuguch@phs.osaka-u.ac.jp*

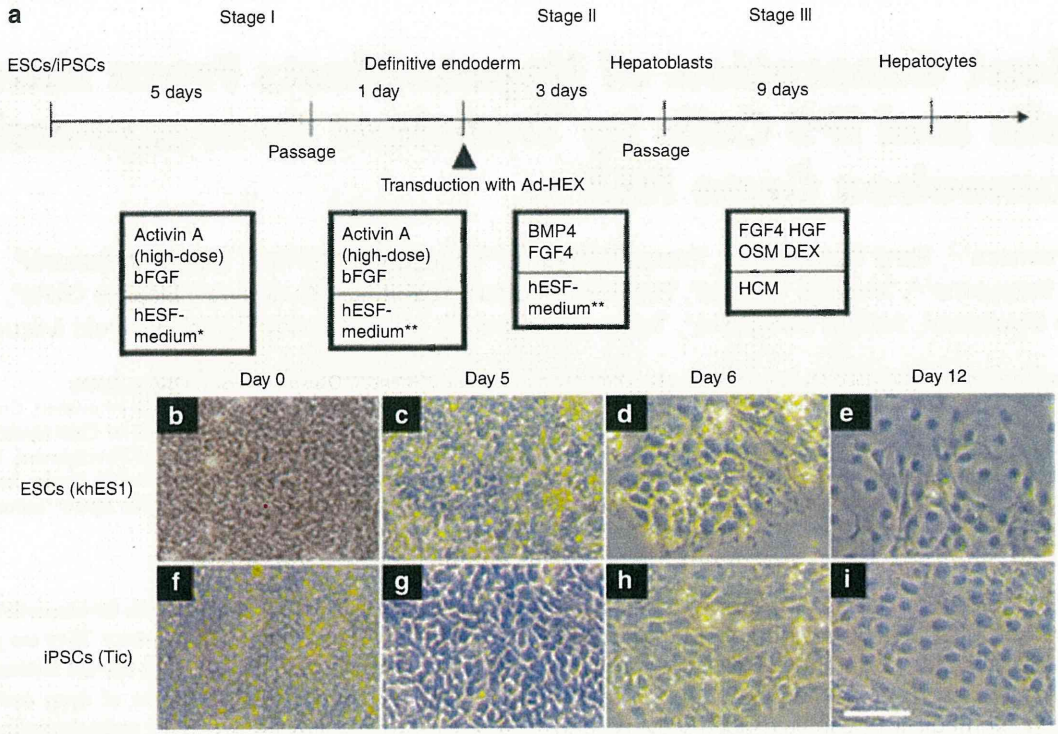

Figure 1 A strategy of differentiation of human embryonic stem cells (ESCs) and induced pluripotent stem cells (iPSCs) to hepatoblasts and hepatocytes. (**a**) Schematic representation illustrating the procedure for differentiation of human ESCs (khES1) and iPSCs (Tic) to hepatocytes. (**b–i**) Phase contrast microscopy showing sequential morphological changes (day 0–12) from (**b–e**) human ESCs (khES1) and (**f–i**) iPSCs (Tic) to hepatoblasts via the definitive endoderm. Bar = 50 µm. bFGF, basic fibroblast growth factor; BMP4, bone morphogenetic protein 4; DEX, dexamethasone; FGF4, fibroblast growth factor 4; HGF, hepatocyte growth factor; OSM, Oncostatin M; HCM, hepatocytes culture medium; *, hESF-GRO medium that was supplemented with 10 µg/ml human recombinant insulin, 5 µg/ml human apotransferrin, 10 µmol/l 2-mercaptoethanol, 10 µmol/l ethanolamine, 10 µmol/l sodium selenite, 0.5 mg/ml fatty acid free BSA; **, hESF-DIF medium that was supplemented with 10 µg/ml insulin, 5 µg/ml apotransferrin, 10 µmol/l 2-mercaptoethanol, 10 µmol/l ethanolamine, 10 µmol/l sodium selenite, 0.5 mg/ml BSA.

of the liver. Although most CYPs (including CYP3A4, CYP7A1, and CYP2D6) are only slightly expressed or not detected in the fetal liver tissue, the expression levels are dramatically increased after birth.[18]

For the development of hepatoblasts, numerous transcription factors are required, such as hematopoietically expressed homeobox (*HEX*), GATA-binding protein 6, prospero homeobox 1, and hepatocyte nuclear factor 4A.[15,19] Among them, *HEX* is suggested to function at the earliest stage of hepatic linage.[20] HEX is first expressed in the definitive endoderm and becomes restricted to the future hepatoblasts. Targeted deletion of the *HEX* gene in the mouse results in embryonic lethality and a dramatic loss of the fetal liver parenchyma.[19,21,22] The hepatic genes, including *ALB*, prospero homeobox1, and hepatocyte nuclear factor 4A, are transiently expressed in the definitive endoderm of *HEX*-null embryos, and further morphogenesis of the hepatoblasts does not occur.[23] In general, then, *HEX* is essential for the definitive endoderm to adopt a hepatic cell fate.

Adenovirus (Ad) vectors are one of the most efficient gene delivery vehicles and have been widely used in both experimental studies and clinical trials.[24] Ad vectors are attractive vehicles for gene transfer because they are easily constructed, can be prepared in high titers, and provide high transduction efficiency in both dividing and nondividing cells. We have developed efficient methods for Ad vector-mediated transient transduction into mouse ESCs and iPSCs.[25,26] We have also showed that the differentiations of mouse ESCs and iPSCs into adipocytes and osteoblasts were dramatically promoted by Ad vector-mediated peroxisome proliferator activated receptor γ and runt related transcription factor 2 transduction, respectively.[25,26]

In this study, we hypothesized that transient *HEX* transduction could efficiently induce hepatoblasts from human ESCs and iPSCs. A previous study demonstrated that *HEX* regulates the differentiation of hemangioblasts and endothelial cells from mouse ESCs,[27] whereas the role of *HEX* in the differentiation of hepatoblasts from human ESCs and iPSCs remains unknown. We found that differentiation of hepatoblasts from the human ESC- and iPSC-derived definitive endoderms, but not from undifferentiated human ESCs and iPSCs, could be facilitated by Ad vector-mediated transient transduction of a *HEX* gene. Furthermore, the Ad-HEX-transduced cells that were derived from human iPSCs were able to differentiate into functional hepatocytes *in vitro*. All the processes for cellular differentiation were performed under serum/feeder cell- free chemically defined conditions. Our culture systems and differentiation method based on Ad vector-mediated transient transduction under chemically defined conditions would provide a platform for drug screening as well as safe therapies.

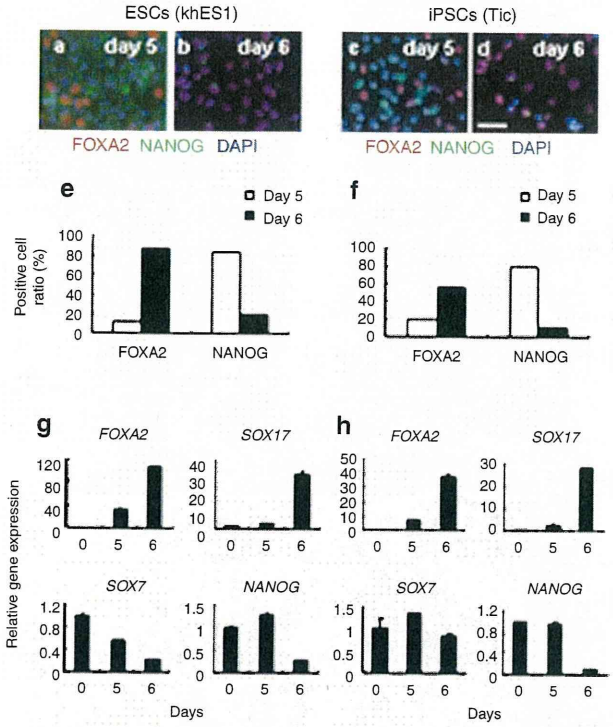

Figure 2 Characterization of the human ESC (khES1)- and iPSC (Tic) derived definitive endoderms. (**a–d**) The immunofluorescent staining of the human ESC (khES1)- and iPSC (Tic) derived differentiated cells before (**a** and **c**; day 5) and after passaging (**b** and **d**; day 6). The cells were immunostained with antibodies against FOXA2 and NANOG. Nuclei were stained with DAPI. (**e**,**f**) Semiquantitative analysis of the immunofluorescent staining in **a–d**. Data are presented as the mean of immunopositive cells counted in eight independent fields. (**g**,**h**) Real-time RT-PCR analysis of the level of definitive endoderm (*FOXA2* and *SOX17*), pluripotent (*NANOG*), and extra-embryonic endoderm (*SOX7*) gene expression at day 5 and 6. At day 5, the cells were passaged. Therefore, the data at day 5 and 6 show the levels of gene expression before (at day 5) or after the passage (at day 6). Data are presented as the mean ± SD from triplicate experiments. The graphs represent the relative gene expression level when the level of undifferentiated cells at day 0 was taken as 1. Bar = 50μm. ESC, embryonic stem cells; iPSC, induced pluripotent stem cells.

RESULTS

Differentiation of human ESC- and iPSC-derived definitive endoderms

Our three-step differentiation protocol is illustrated in **Figure 1a**. After treatment with 50 ng/ml of Activin A (high-dose) and basic fibroblast growth factor (bFGF) for 5 days on a laminin-coated plate, morphologically, the human ESCs and iPSCs were gradually transformed from typical, defined, tight human ESC, and iPSC colonies (day 0) into less dense, flatter cells containing prominent nuclei (day 5), even though the majority of the cells had a morphology resembling that of undifferentiated cells (**Figure 1b,c,f,g**). FACS analysis showed that ~46% of human iPSC-derived differentiated cells expressed CXCR4 (expressed in the definitive endoderm but not the primitive endoderm) (**Supplementary Figure S1a**). Human ESC- and iPSC-derived differentiated cells were immunostained with the definitive endoderm marker, FOXA2 (**Figure 2a,c**). However, the majority of the cells expressed the pluripotent marker NANOG, indicating that undifferentiated cells remain in the induced cultures at day 5. After the cells were passaged with trypsin-EDTA and seeded on a laminin-coated plate a second time, the resultant cells were found to be more homogeneous and flatter at day 6 (**Figure 1d,h**). Semiquantitative analysis by counting immunopositive cells revealed that the number of FOXA2-positive cells was increased and, in turn, the number of NANOG-positive cells was decreased at day 6 after passaging (**Figure 2e,f**). Real-time reverse transcriptase (RT)-PCR analysis showed that the definitive endoderm markers *FOXA2* and *SOX17* mRNA were upregulated, whereas the pluripotent marker *NANOG* mRNA was downregulated at day 6 (**Figure 2g,h**). These results were consistent with the immunofluorescence results (**Figure 2a–d**). The expression levels of the mesoderm marker *FLK1* mRNA and ectoderm marker *PAX6* mRNA were downregulated or unchanged at day 6 (**Supplementary Figure S1b–e**). Importantly, the expression of *SOX7* mRNA (expressed in the extra-embryonic endoderm but not the definitive endoderm) was downregulated (**Figure 2g,h**). These results indicate that the definitive endoderm is induced or selected from human ESCs and iPSCs after passaging. We obtained the same results using another human iPSC line (**Supplementary Figure S2a–d**).

HEX induces hepatoblasts from the human ESC- and iPSC-derived definitive endoderms

To investigate whether forced expression of transcription factors could promote hepatic differentiation, the human ESC- and iPSC-derived definitive endoderms were transduced with Ad vectors. We used a fiber-modified Ad vector containing the elongation factor-1α promoter and a stretch of lysine residue (K7) peptides in the C-terminal region of the fiber knob to examine the transduction efficiency in the human ESC- and iPSC-derived definitive endoderms. The elongation factor-1α promoter was found to be highly active in human ESCs.[28] The K7 peptide targets heparan sulfates on the cellular surface, and the fiber-modified Ad vector containing K7 peptides was shown to be efficient for transduction into many kinds of cells.[29,30] The human ESC- and iPSC-derived definitive endoderms were transduced with a LacZ-expressing Ad vector (Ad-LacZ) at 3,000 vector particle/cell. X-Gal staining showed that the Ad-LacZ-transduced human ESC- and iPSC-derived definitive endoderms successfully expressed LacZ (**Figure 3**). Nearly 100% of the cells transduced with Ad-LacZ were strongly X-gal positive. The transduction efficiency in the human ESC- and iPSC-derived definitive endoderms transduced with the conventional Ad vector containing the wild-type capsid at 3,000 vector particle/cell was ~80% and X-gal staining was much weaker than that in the cells transduced with fiber-modified Ad vectors (**Supplementary Figure S6**).

Next, the human ESC- and iPSC-derived definitive endoderms were transduced with a HEX-expressing fiber-modified Ad vector (Ad-HEX). Although HEX is known to be a transcription factor that is essential for liver development, it remains unclear what the effect of transient *HEX* overexpression is on differentiation from human ESCs and iPSCs or their derivatives *in vitro*. We confirmed the overexpression of *HEX* in the human ESC- and iPSC-derived definitive endoderms transduced with Ad-HEX (**Supplementary Figure S3a–f**). Gene expression analysis revealed the upregulation of *AFP* mRNA, which was expressed by hepatoblasts or early hepatocytes, in Ad-HEX-transduced cells as

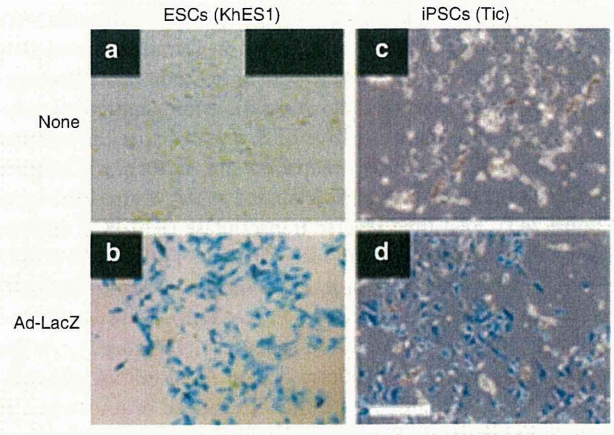

Figure 3 Efficient transgene expression in the human ESC (khES1)- and iPSC (Tic) derived definitive endoderms by using a fiber-modified Ad vector containing the EF-1α promoter. (**a,b**) Human ESC (khES1)-derived and (**c,d**) iPSC (Tic) derived definitive endoderms were transduced with 3,000 VP/cell of Ad-LacZ for 1.5 hours. The next day after transduction, X-gal staining was performed as described in the Materials and Methods section. Similar results were obtained in two independent experiments. Scale = 50 μm. Ad, adenovirus; EF-1α, elongation factor-1α; ESC, embryonic stem cells; iPSC, induced pluripotent stem cells; LacZ, Ad-LacZ-transduced cells; None, nontransduced cells.

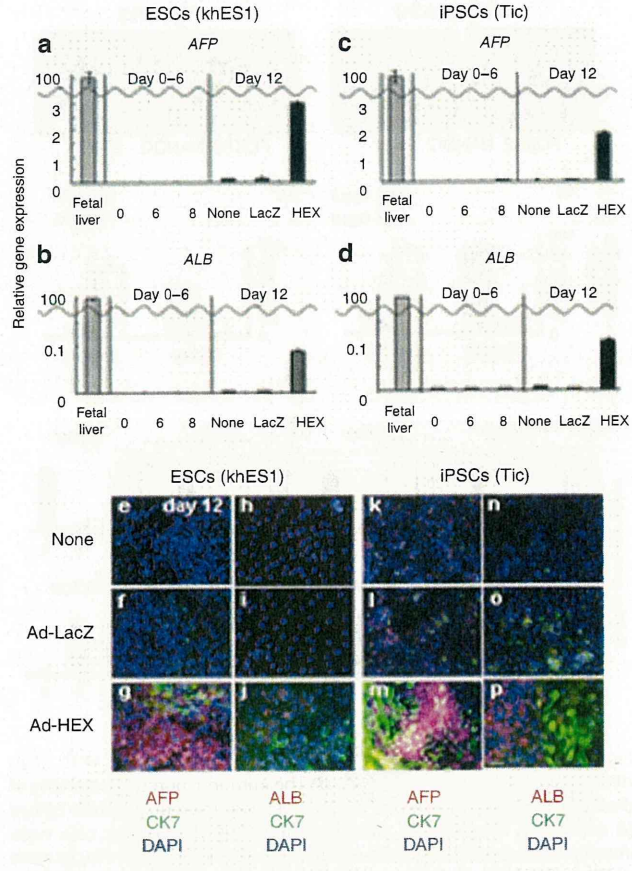

Figure 4 Efficient hepatoblast differentiation from the human ESC (khES1)- and iPSC (Tic) derived definitive endoderms by transduction of the *HEX* gene. (**a–d**) Real-time RT-PCR analysis of the level of (**a,c**) *AFP* and (**b,d**) *ALB* expression in nontransduced cells, Ad-LacZ-transduced cells, and Ad-HEX-transduced cells, all of which were induced from the human ESC (khES1)- and iPSC (Tic) derived definitive endoderms (day 0, 5, 6, and 12). The cells were transduced with Ad-LacZ or Ad-HEX at day 6 as described in **Figure 1a**. The data at day 6 was obtained before the transduction with Ad-HEX. The graphs represent the relative gene expression levels when the level in the fetal liver was taken as 100. (**e–p**) Immunocytochemistry of AFP, ALB, and CK7 expression in nontransduced cells (**e,h,k,** and **n**), Ad-LacZ-transduced cells (**f,i,l,** and **o**), and Ad-HEX-transduced cells (**g,j,m,** and **p**) at day 12, all of which were induced from the human ESC (khES1)- and iPSC (Tic) derived definitive endoderms. Nuclei were stained with DAPI. Bar = 50 μm. Ad, adenovirus; AFP, α-fetoprotein; ALB, albumin; CK7, cytokeratin 7; HEX, Ad-HEX-transduced cells; ESC, embryonic stem cells; iPSC, induced pluripotent stem cell; LacZ, Ad-LacZ-transduced cells; None, nontransduced cells.

compared with nontransduced cells or Ad-LacZ-transduced cells (**Figure 4a,c**). Expression of *ALB* mRNA, which is the most abundant protein in liver, was also observed in Ad-HEX-transduced cells (**Figure 4b,d**).

During liver development, both hepatocytes and cholangiocytes were differentiated from the hepatoblasts. We examined the protein expression of AFP, ALB, and the cholangiocyte marker cytokeratin 7 (CK7) in Ad-HEX-transduced cells by immunostaining (**Figure 4e–p**). The AFP-positive populations were detected in Ad-HEX-transduced cells (**Figure 4g,m**). ALB-positive cells were also detected, although the detection efficiency was very low (**Figure 4j,p**). CK7-positive cells were observed among the Ad-HEX-transduced cells, and all CK7-positive cells were found near the AFP- and ALB-positive cells, suggesting that hepatoblasts are generated by the transient overexpression of a *HEX* gene. Semiquantitative RT-PCR analysis showed that the expression levels of the liver-enriched transcription factors hepatocyte nuclear factor 1A, hepatocyte nuclear factor 1B, hepatocyte nuclear factor 4A, and hepatocyte nuclear factor 6 mRNA were upregulated in Ad-HEX-transduced cells (**Supplementary Figure S4a,b**). The expressions of CCAAT/enhancer binding protein α and prospero homeobox 1 mRNA, two transcription factors known to play a pivotal role in the establishment of the hepatoblasts, were also induced in Ad-HEX-transduced cells (**Supplementary Figure S4a, b**). Taken together, these findings indicate that *HEX* enhances the specification of hepatoblasts from the human ESC- and iPSC-derived definitive endoderms. Similar results were obtained with another human iPSC line (**Supplementary Figure S2e–g**).

Time course of differentiation of the definitive endoderm to hepatoblasts

Next, we examined the time course of AFP and CK7 expression during differentiation of human iPSCs to hepatoblasts in Ad-HEX-transduced cells and nontransduced cells. At day 7 (the day after transduction), the expression of AFP was not detectable in Ad-HEX-transduced or nontransduced cells (**Supplementary Figure S5a,d**). At day 8–9, morphological changes to hepatocyte-like cells were observed in Ad-HEX-transduced cells (**Supplementary Figure S5h,i**). We also observed homogeneous AFP-positive cells at day 9 (**Supplementary Figure S5e**). At day 10, CK7-positive cells appeared, indicating that hepatoblasts started to differentiate into hepatocytes and cholangiocytes at day 9–10 (**Supplementary Figure S5f**). At day 12, ALB-positive cells appeared, indicating that hepatocytes were differentiated from Ad-HEX-transduced cells (**Figure 4p**). These results showed that *HEX* induces the hepatoblasts from the

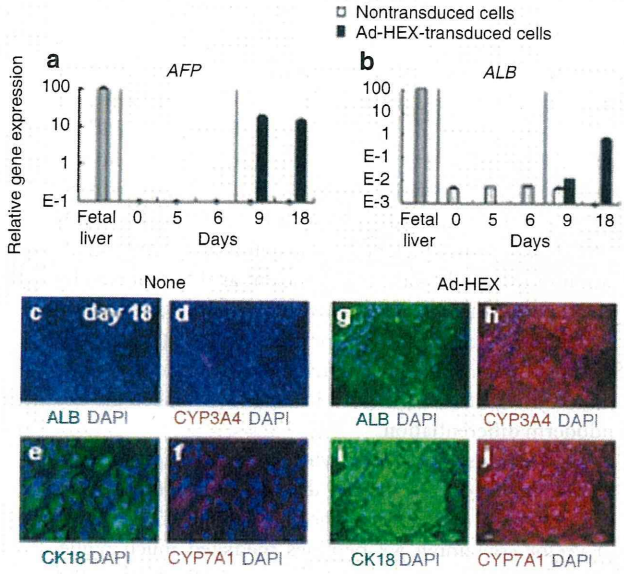

Figure 5 Efficient differentiation of Ad-HEX-transduced hepatoblasts into hepatocytes. (**a**,**b**) Real-time RT-PCR analysis of (**a**) *AFP* and (**b**) *ALB* expression in nontransduced cells and Ad-HEX-transduced cells, both of which were induced from the human iPSC (Tic) derived definitive endoderm (day 0, 5, 6, and 12). The cells were transduced with Ad-HEX at day 6 as described in **Figure 1a**. The data at day 6 were obtained before the transduction with Ad-HEX. The graphs represent the relative gene expression level when the level in the fetal liver was taken as 100. (**c–j**) Immunocytochemistry of ALB, CYP3A4, CYP7A1, and CK18 expression in (**c–f**) nontransduced cells and (**g–j**) Ad-HEX-transduced cells, all of which were induced from the human iPSC (Tic) derived definitive endoderm at day 18. Nuclei were stained with DAPI. Bar = 50 μm. Ad, adenovirus; AFP, α-fetoprotein; ALB, albumin; CK18, cytokeratin 18; ESC, embryonic stem cells; HEX, Ad-HEX-transduced cells; iPSC, induced pluripotent stem cell; None, nontransduced cells; RT-PCR, reverse transcriptase-PCR.

definitive endoderm, and the Ad-HEX-transduced cells could differentiate into both hepatocytes and cholangiocytes.

Directed hepatic differentiation from hepatoblasts

With the protocol described above, heterogeneous populations containing CK7-positive cholangiocytes were observed at day 12 (**Figure 4p**). To promote the differentiation of hepatoblasts to hepatocytes, the human iPSC-derived differentiated cells at day 9 (**Supplementary Figure S5e**) were dislodged with trypsin-EDTA and plated on collagen I-coated dishes as previously reported.[11] After 8–11 days in culture with medium containing FGF4, HGF, OSM, and DEX, the Ad-HEX-transduced cells became more flattened (**Supplementary Figure S5m**), whereas the nontransduced cells became fibroblast-like cells (**Supplementary Figure S5i**). Gene expression analysis showed the upregulation of *ALB* mRNA in Ad-HEX-transduced cells under this culture condition, whereas the expression of *ALB* mRNA was reduced in the nontransduced cells at day 18 (**Figure 5b**). Immunostaining showed that only a small percentage of Ad-HEX-transduced cells expressed ALB at day 12 (**Figure 4p**), whereas most of the Ad-HEX-transduced cells were ALB-positive at day 18 (**Figure 5g**). Most of the Ad-HEX-transduced cells also expressed CYP3A4 at day 18 (**Figure 5h**). More importantly, in the Ad-HEX-transduced cells, CYP7A1 and cytokeratin 18 were detected and these proteins are known

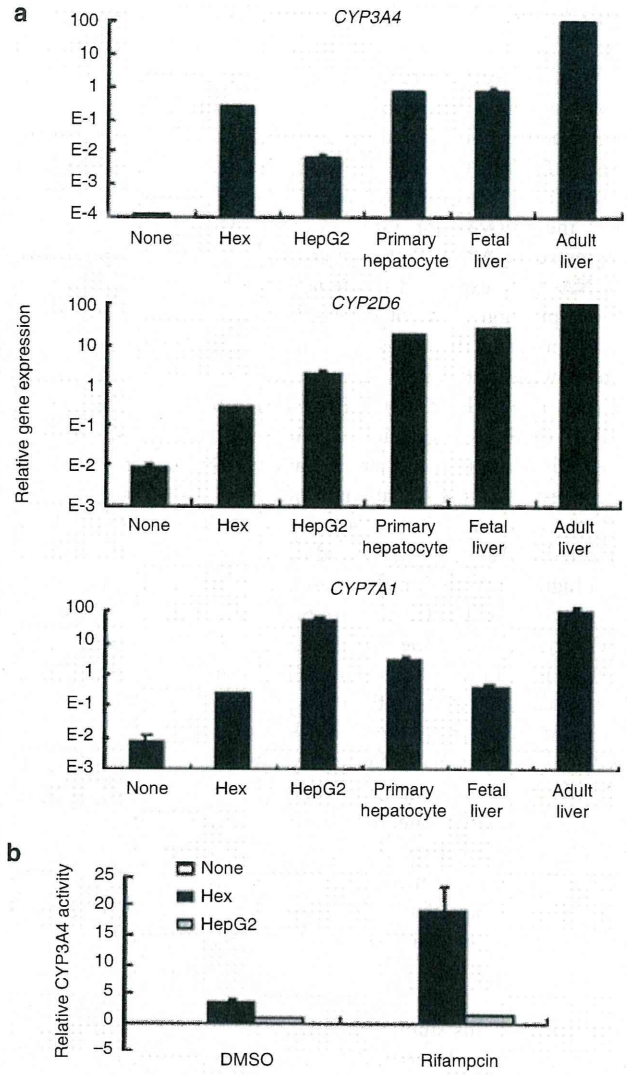

Figure 6 Cytochrome P450 isozymes in human iPSC (Tic) derived hepatocytes. (**a**) Real-time RT-PCR analysis of *CYP3A4*, *CYP7A1*, and *CYP2D6* expression in iPSC (Tic) derived nontransduced cells, Ad-HEX-transduced cells, and fetal and adult liver tissues. (**b**) Induction of CYP3A4 by rifampicin in human iPSC (Tic) derived nontransduced cells, Ad-HEX-transduced cells, the HepG2 cell line and primary human hepatocytes, which were cultured 48 hours after plating the cells. Data are presented as the mean ± SD from triplicate experiments. The graphs represent the relative gene expression level when the level in the adult liver was taken as 100. AFP, α-fetoprotein; ALB, albumin; DMSO, dimethyl sulfoxide; ESC, embryonic stem cells; HEX, Ad-HEX-transduced cells; iPSC, induced pluripotent stem cell; LacZ, Ad-LacZ-transduced cells; None, nontransduced cells.

to be detected in hepatocytes but not in extra-embryonic cells[31,32] (**Figure 5i,j**). Quantitative analysis showed that ~84, 80, 88, and 92% of Ad-HEX-transduced cells expressed ALB, CYP3A4, CYP7A1, and cytokeratin 18, respectively. These results indicate that Ad-HEX-transduced cells could differentiate to hepatic cells. However, the expression level of *ALB* mRNA in Ad-HEX-transduced cells was lower than that in fetal liver tissue and in turn, the expression of *AFP* mRNA was maintained (**Figure 5a**). Therefore, Ad-HEX-transduced cells are committed to the hepatic linage, but are not yet mature hepatocytes.

Ad-HEX-transduced cells exhibit hepatic functions

To test the hepatic function in the Ad-HEX-transduced cells, we investigated the liver metabolism, because P450 cytochrome enzymes play a critical role in this function. We examined the expression level of several members of this multigene family, *i.e.*, *CYP3A4*, *CYP7A1*, mRNA and *CYP2D6* in Ad-HEX-transduced cells by real-time RT-PCR. The real-time RT-PCR analysis showed that the mRNAs for *CYP3A4*, *CYP7A1*, and *CYP2D6* were expressed in Ad-HEX-transduced cells, whereas none of these mRNAs were expressed in the nontransduced cells (**Figure 6a**). The expression levels of *CYP3A4* in Ad-HEX-transduced cells were similar to those observed in primary human hepatocytes, which were cultured 48 hours after plating the cells, or fetal liver tissues but lower than those in adult liver. The *CYP2D6* and *CYP7A1* mRNA expressions in Ad-HEX-transduced cells were lower than those in primary hepatocytes or adult tissues. Next, we investigated the metabolism of the P450 3A4 substrates by measuring the activity of P450 isozymes. The metabolites were detected in Ad-HEX-transduced cells, and their activity was 3.4-fold higher than that in the most commonly used human hepatocyte cell line, HepG2 (**Figure 6b**; DMSO column). This result was consistent with the real-time RT-PCR data (**Figure 6a**). We further tested the induction of CYP3A4 upon chemical stimulation, because CYP3A4 is the most prevalent P450 isozyme in the liver and is involved in the metabolism of a significant proportion of the currently available commercial drugs. Because CYP3A4 can be induced with rifampicin, both Ad-HEX-transduced cells and HepG2 cells were treated with rifampicin, followed by treatment with CYP3A4 substrate. Ad-HEX-transduced cells produced 5.4-fold higher levels of metabolites in response to rifampicin treatment (**Figure 6b**; rifampicin column). This result indicates that P450 isozymes are active in Ad-HEX-transduced cells.

DISCUSSION

The object of this study was to develop an efficient method for generating hepatoblasts and hepatocytes from human ESCs and iPSCs for application to drug toxicity screening tests as well as therapeutics such as regenerative medicine. We found that transient HEX transduction in the definitive endoderm together with a culture under chemically defined conditions was useful for this purpose.

It has been reported that a high concentration of Activin A induces differentiation of human ESCs into the definitive endoderm.[8,33,34] On the other hand, undifferentiated human ESCs are maintained by a low concentration of Activin A.[35] Several studies have shown that bFGF promotes the differentiation of ESCs into the definitive endoderm and inhibits the differentiation of ESCs into the extra-embryonic endoderm.[35–38] bFGF has been reported to inhibit the BMP signaling, which can promote the extra-embryonic lineage differentiation.[39] The extra-embryonic endoderm expresses most of the hepatocyte markers, such as AFP.[40] Contamination of the extra-embryonic endoderm makes it difficult to estimate the hepatic differentiation from human ESCs and iPSCs.[11,14,40] In this study, we showed that both Activin A and bFGF induce definitive endoderm populations, while they repress the extra-embryonic endoderm differentiation (**Figure 2g,h**). Interestingly, after the differentiated cells that were cultured on laminin-coated plates with Activin A and bFGF were passaged at day 5, FOXA2-positive cells (definitive endoderm) were enriched in the resultant cells at day 6 (**Figure 2a–f**). This may have been because FOXA2-positive cells efficiently adhered to the laminin-coated plate and/or because trypsinized, single undifferentiated ESCs/iPSCs cannot survive. The passaging of differentiated cells might be attributed to the reduction in the number of not only the extra-embryonic endoderm cells but also the undifferentiated cells. However, the efficiency of the definitive endoderm differentiation in this study was not as efficient as that reported by other groups.[8,33,34] Other cell lineages, such as the mesoderm and extra-embryonic endoderm, might remain at day 6 (**Figure 2g,h** and **Supplementary Figure S1**). Further improvement of the culture conditions will thus be needed in order to enhance the definitive endoderm differentiation.

Hepatoblasts and hepatocytes were differentiated from the human ESC- and iPSC-derived definitive endoderms by transient overexpression of the homeobox gene *HEX*. A fiber-modified Ad vector containing K7 peptides mediated much higher gene expression than conventional Ad vectors in the human ESC- and iPSC-derived definitive endoderms (**Supplementary Figure S6**). This new hepatic differentiation protocol shows that *HEX* induces AFP-positive hepatoblasts at day 9 and ALB-positive hepatocytes at day 12 from human ESCs and iPSCs, whereas the previous protocols require a few weeks or months to induce AFP- and ALB-positive hepatocytes from PSCs.[9–11] Previous studies suggested that *HEX* could regulate liver-enriched transcription factors such as hepatocyte nuclear factor 4A and hepatocyte nuclear factor 6.[19,23] Overexpression of the *HEX* gene under the conditions employed in the present study could activate several transcription factors that are required for hepatic differentiation (**Supplementary Figure S4a,b**). However, the Ad-HEX-transduced cells showed a low level of expression of *ALB* and some CYP450 species, as well as a high level of *AFP* expression, indicating that the cells were still immature. To promote further hepatic differentiation or maturation, it may be effective to culture the hepatic cells in a 3D environment or on feeder cells such as cardiomyocyte- or endothelium-derived cells.[41,42] In addition, the function of our hepatic cells was still limited. Further analysis of the other functions of our hepatic cells, such as glycogen storage, uptake of indocyanine green and organic anion low-density lipoprotein, and transplantation of Ad-HEX-transduced cells into the liver of immunodeficient mice, is clearly needed for the appreciation to drug screening and therapeutic treatment modalities.

During the preparation of this article, Kubo *et al.* have reported that *HEX* could promote hepatoblast differentiation from mouse ESCs.[43] Their report is consistent with our data, suggesting that *HEX* plays a pivotal regulatory role in not only mouse but also human hepatic differentiation. They also showed that the overexpression of *HEX* at the definitive endoderm stage is critical for hepatic specification of the mouse ESCs. We also confirmed that forced expression of *HEX* in the undifferentiated human ESCs and iPSCs did not elevate the expression of *ALB* and *CK7* (**Supplementary Figure S7**), indicating that *HEX* enhances the hepatic differentiation not from the undifferentiated cells but from the definitive endoderm. However, Kubo *et al.* used recombinant mouse ESCs (tet-HEX ESCs), in which the tetracycline-regulated *HEX* expression cassette

is integrated into the host cell genome to induce *HEX* in a stage-specific manner. Their system would not be appropriate for clinical use because the transgene is randomly integrated into the host cell genome and this leads to a risk of mutagenesis.[44] On the other hand, we generated human hepatoblasts by Ad vector-mediated transient *HEX* transduction, method which avoids the integration of exogenous DNA into the host chromosome.

Touboul *et al.* reported that human ESCs and iPSCs can differentiate into functional hepatocytes under chemically defined conditions.[34] In the present study, hepatoblasts were generated in a chemically defined serum-free medium, which minimized exposure to animal cells and proteins, and on a defined extracellular matrix, such as laminin or collagen, which do not contain undefined growth factors. To generate hepatocytes, hepatocyte culture medium, which is serum-free but not defined, was used in the stage III. When defined hESF-medium was used in the stage III, the expression levels of *ALB* and *CYP3A4* mRNA were half the levels seen in the cells cultured with hepatocyte culture medium in the preliminary experiment (data not shown). Human ESCs and iPSCs were also grown for maintaining the undifferentiated state on a feeder layer, which contains xenoantigen such as bovine apolipoprotein B-100. Bovine apolipoprotein B-100 is known to be a dominant xenoantigen for cell-based therapies.[45] Human ESC- and iPSC-derived hepatocytes should be generated and cultured under chemically defined conditions not only to avoid potential contamination with pathogens for the safer therapeutic application, but also to obtain reproducible results using the differentiation protocols.[34,46] Development of differentiation protocols using other genes of transcription factors as well as *HEX* genes based on a chemically defined medium is under way. Overall, our strategy should provide a novel protocol for hepatic differentiation from human ESCs and iPSCs, which could be useful for regenerative medicine and drug screening.

MATERIALS AND METHODS

Ad vectors. Ad vectors were constructed by an improved *in vitro* ligation method.[47,48] The human *HEX* complementary DNA derived from pDNR-LIB-*HEX* (Invitrogen, Carlsbad, CA) was inserted into pHMEF5,[29] which contains the human elongation factor-1α promoter, resulting in pHMEF-HEX. The pHMEF-HEX was digested with I-CeuI/PI-SceI and ligated into I-CeuI/PI-SceI-digested pAdHM41-K7,[30] resulting in pAd-HEX. Ad-HEX and Ad-LacZ, both of which contain the elongation factor-1α promoter and a stretch of lysine residues (K7) peptides in the C-terminal region of the fiber knob, were generated and purified as described previously.[26,29] The vector particle titer was determined by using a spectrophotometric method.[49]

Human ESCs and iPSCs culture. A human ESC line, khES1, was obtained from Kyoto University (Kyoto, Japan).[50] khES1 was used following the Guidelines for Derivation and Utilization of Human Embryonic Stem Cells of the Ministry of Education, Culture, Sports, Science and Technology of Japan after approval by the review board at Kyoto University. Human ESCs were maintained on a feeder layer of mitomycin-inactivated mouse embryonic fibroblasts (ICR; ReproCELL Incorporated, Tokyo, Japan) with Dulbecco's modified Eagle's medium/F-12 (Sigma, St Louis, MO) supplemented with 0.1 mmol/l 2-mercaptoethanol, 0.1 mmol/l nonessential amino acids, 2 mmol/l L-glutamine, 20% GIBCO knockout serum replacement (Invitrogen), and 5 ng/ml bFGF (Sigma) in a humidified atmosphere of 3% CO_2 and 97% air at 37 °C. Human ESCs were dissociated with 0.1 mg/ml dispase (Roche Diagnostics, Burgess Hill, UK) into small clumps, and subcultured every 5 or 6 days.

Two human iPS clones derived from the embryonic human lung fibroblast cell line MCR5 were provided from JCRB Cell Bank (Tic, JCRB Number: JCRB1331; and Dotcom, JCRB Number: JCRB1327).[3,4] In the present study, we mainly used the Tic cell line, but similar results were obtained using the Dotcom cell line, and these are shown in the supplementary figures. Human iPSCs were maintained on a feeder layer of mitomycin-inactivated mouse embryonic fibroblasts (Hygro Resistant Strain C57/BL6; Hygro, Millipore, MA) on a gelatin-coated flask in human iPS medium. Human iPS medium consists of knockout Dulbecco's modified Eagle's medium/F12 (Invitrogen), supplemented with 0.1 mmol/l 2-mercaptoethanol, 0.1 mmol/l nonessential amino acids, 2 mmol/l L-glutamine, 20% knockout serum replacement, and 10 ng/ml bFGF in a humidified atmosphere of 5% CO_2 and 95% air at 37 °C. Human iPSCs were dissociated with 0.1 mg/ml dispase (Roche) into small clumps and subcultured every 7 or 8 days.

In vitro *differentiation.* Before the initiation of cellular differentiation, the medium of human ESCs and iPSCs was exchanged for a defined serum-free medium hESF9 and cultured in a humidified atmosphere of 10% CO_2 and 90% air at 37 °C.[46] hESF9 consists of hESF-GRO medium (Cell Science & Technology Institute, Sendai, Japan) supplemented with five factors (10 μg/ml human recombinant insulin, 5 μg/ml human apotransferrin, 10 μmol/l 2-mercaptoethanol, 10 μmol/l ethanolamine, 10 μmol/l sodium selenite), oleic acid conjugated with fatty acid free bovine ALB, 10 ng/ml bFGF, and 100 ng/ml heparin (all from Sigma). For induction of definitive endoderm, human ESCs and iPSCs were dissociated into single cells with Accutase (Invitrogen) and cultured for 5 days on a mouse laminin-coated tissue 12-well plate (6.0×10^4 cells/cm^2) in hESF-GRO medium (Cell Science & Technology Institute) supplemented with the five factors, 0.5 mg/ml fatty acid free bovine ALB (BSA) (Sigma), 10 ng/ml bFGF, and 50 ng/ml Activin A (R&D Systems, Minneapolis, MN) in a humidified atmosphere of 10% CO_2 and 90% air at 37 °C. The medium was refreshed every day.

For induction of hepatoblasts, the human ESC- and iPSC-derived definitive endoderms (day 5) were dissociated with 0.0125% trypsin-0.01325 mmol/l EDTA, and then the trypsin was inactivated with 0.1% soybean trypsin inhibitor (Sigma). The cells were seeded at 1.2×10^5 cells/cm^2 on a laminin-coated 12-well plate with hESF-DIF (Cell Science & Technology Institute) medium supplemented with the five factors, 0.5 mg/ml BSA, 10 ng/ml bFGF, and 50 ng/ml Activin A in a humidified atmosphere of 10% CO_2 and 90% air at 37 °C. The next day, the cells were transduced with 3,000 vector particle/cell of Ad vectors (Ad-HEX and Ad-LacZ) for 1.5 hours in hESF-DIF medium supplemented with the five factors, BSA, 10 ng/ml FGF4 (R&D Systems) and 10 ng/ml BMP4 (R&D Systems).[10] The medium was refreshed every day.

For induction of hepatocytes, human iPSC-derived hepatoblasts in one well (day 9) were passaged onto two wells with 0.0125% trypsin-0.01325mmol/l EDTA and 0.1% trypsin inhibitor, on type I collagen-coated tissue 12-well plate (15 μg/cm^2) (Nitta Gelatin, Osaka, Japan). The cells were cultured in hepatocyte culture medium supplemented with SingleQuots (Lonza, Walkersville, MD), 10 ng/ml FGF4, 10 ng/ml HGF (R&D Systems), 10 ng/ml Oncostatin M (R&D Systems), and 0.392 ng/ml dexamethasone (Sigma).[11] The medium was refreshed every 2 days.

RNA isolation, RT-PCR, immunostaining, flow cytometry, lacz assay, and assay for cytochrome P4503A4 activity. For details of these procedures, See **Supplementary Materials and Methods**, **Supplementary Tables S1 and S2.**

SUPPLEMENTARY MATERIAL

Figure S1. Characterization of the human ESC (khES1)- and iPSC (Tic)-derived definitive endoderms.

Figure S2. Efficient differentiation of another human iPSC line (Dotcom) into hepatoblasts by overexpression of the *HEX* gene.

Figure S3. Overexpression of *HEX* in the human ESC (khES1)- and iPSC (Tic)-derived definitive endoderms.

Figure S4. Characterization of Ad-HEX-transduced hepatoblasts.
Figure S5. Progression of differentiation of the definitive endoderm to hepatoblasts.
Figure S6. X-gal staining of human iPSC (Tic)-derived definitive endoderms transduced with a conventional or a fiber-modified Ad vector containing the EF-1α promoter.
Figure S7. *HEX* promotes the differentiation into the hepatic lineage, not from undifferentiated iPSCs (Tic), but from iPSC (Tic)-derived definitive endoderm.
Table S1. List of Taqman gene expression assays and primers.
Table S2. List of antibodies used.
Materials and Methods.

ACKNOWLEDGMENTS

We thank Hiroko Matsumura and Midori Hayashida for their excellent technical support. This study was supported by grants from the Ministry of Education, Sports, Science and Technology of Japan (20200076) and by grants from the Ministry of Health, Labor, and Welfare of Japan.

REFERENCES

1. Thomson, JA, Itskovitz-Eldor, J, Shapiro, SS, Waknitz, MA, Swiergiel, JJ, Marshall, VS *et al.* (1998). Embryonic stem cell lines derived from human blastocysts. *Science* **282**: 1145–1147.
2. Takahashi, K, Tanabe, K, Ohnuki, M, Narita, M, Ichisaka, T, Tomoda, K *et al.* (2007). Induction of pluripotent stem cells from adult human fibroblasts by defined factors. *Cell* **131**: 861–872.
3. Makino, H, Toyoda, M, Matsumoto, K, Saito, H, Nishino, K, Fukawatase, Y *et al.* (2009). Mesenchymal to embryonic incomplete transition of human cells by chimeric OCT4/3 (POU5F1) with physiological co-activator EWS. *Exp Cell Res* **315**: 2727–2740.
4. Nagata, TM, Yamaguchi, S, Hirano, K, Makino, H, Nishino, K, Miyagawa, Y *et al.* (2009). Efficient reprogramming of human and mouse primary extra-embryonic cells to pluripotent stem cells. *Genes Cells* **14**: 1395–1404.
5. Lavon, N and Benvenisty, N (2005). Study of hepatocyte differentiation using embryonic stem cells. *J Cell Biochem* **96**: 1193–1202.
6. Khetani, SR and Bhatia, SN (2008). Microscale culture of human liver cells for drug development. *Nat Biotechnol* **26**: 120–126.
7. Baharvand, H, Hashemi, SM and Shahsavani, M (2008). Differentiation of human embryonic stem cells into functional hepatocyte-like cells in a serum-free adherent culture condition. *Differentiation* **76**: 465–477.
8. Hay, DC, Zhao, D, Fletcher, J, Hewitt, ZA, McLean, D, Urruticoechea-Uriguen, A *et al.* (2008). Efficient differentiation of hepatocytes from human embryonic stem cells exhibiting markers recapitulating liver development in vivo. *Stem Cells* **26**: 894–902.
9. Shiraki, N, Umeda, K, Sakashita, N, Takeya, M, Kume, K and Kume, S (2008). Differentiation of mouse and human embryonic stem cells into hepatic lineages. *Genes Cells* **13**: 731–746.
10. Song, Z, Cai, J, Liu, Y, Zhao, D, Yong, J, Duo, S *et al.* (2009). Efficient generation of hepatocyte-like cells from human induced pluripotent stem cells. *Cell Res* **19**: 1233–1242.
11. Agarwal, S, Holton, KL and Lanza, R (2008). Efficient differentiation of functional hepatocytes from human embryonic stem cells. *Stem Cells* **26**: 1117–1127.
12. Si-Tayeb, K, Noto, FK, Nagaoka, M, Li, J, Battle, MA, Duris, C *et al.* (2010). Highly efficient generation of human hepatocyte-like cells from induced pluripotent stem cells. *Hepatology* **51**: 297–305.
13. Duan, Y, Ma, X, Zou, W, Wang, C, Bahbahan, IS, Ahuja, TP *et al.* (2010). Differentiation and characterization of metabolically functioning hepatocytes from human embryonic stem cells. *Stem Cells* **28**: 674–686.
14. Cai, J, Zhao, Y, Liu, Y, Ye, F, Song, Z, Qin, H *et al.* (2007). Directed differentiation of human embryonic stem cells into functional hepatic cells. *Hepatology* **45**: 1229–1239.
15. McLin, VA and Zorn, AM (2006). Molecular control of liver development. *Clin Liver Dis* **10**: 1–25, v.
16. Shiojiri, N (1981). Enzymo- and immunocytochemical analyses of the differentiation of liver cells in the prenatal mouse. *J Embryol Exp Morphol* **62**: 139–152.
17. Shiojiri, N (1984). The origin of intrahepatic bile duct cells in the mouse. *J Embryol Exp Morphol* **79**: 25–39.
18. Ingelman-Sundberg, M, Oscarson, M and McLellan, RA (1999). Polymorphic human cytochrome P450 enzymes: an opportunity for individualized drug treatment. *Trends Pharmacol Sci* **20**: 342–349.
19. Hunter, MP, Wilson, CM, Jiang, X, Cong, R, Vasavada, H, Kaestner, KH *et al.* (2007). The homeobox gene Hhex is essential for proper hepatoblast differentiation and bile duct morphogenesis. *Dev Biol* **308**: 355–367.
20. Bogue, CW, Ganea, GR, Sturm, E, Ianucci, R and Jacobs, HC (2000). Hex expression suggests a role in the development and function of organs derived from foregut endoderm. *Dev Dyn* **219**: 84–89.
21. Martinez Barbera, JP, Clements, M, Thomas, P, Rodriguez, T, Meloy, D, Kioussis, D *et al.* (2000). The homeobox gene Hex is required in definitive endodermal tissues for normal forebrain, liver and thyroid formation. *Development* **127**: 2433–2445.
22. Keng, VW, Yagi, H, Ikawa, M, Nagano, T, Myint, Z, Yamada, K *et al.* (2000). Homeobox gene Hex is essential for onset of mouse embryonic liver development and differentiation of the monocyte lineage. *Biochem Biophys Res Commun* **276**: 1155–1161.
23. Bort, R, Signore, M, Tremblay, K, Martinez Barbera, JP and Zaret, KS (2006). Hex homeobox gene controls the transition of the endoderm to a pseudostratified, cell emergent epithelium for liver bud development. *Dev Biol* **290**: 44–56.
24. Xu, ZL, Mizuguchi, H, Sakurai, F, Koizumi, N, Hosono, T, Kawabata, K *et al.* (2005). Approaches to improving the kinetics of adenovirus-delivered genes and gene products. *Adv Drug Deliv Rev* **57**: 781–802.
25. Tashiro, K, Inamura, M, Kawabata, K, Sakurai, F, Yamanishi, K, Hayakawa, T *et al.* (2009). Efficient adipocyte and osteoblast differentiation from mouse induced pluripotent stem cells by adenoviral transduction. *Stem Cells* **27**: 1802–1811.
26. Tashiro, K, Kawabata, K, Sakurai, H, Kurachi, S, Sakurai, F, Yamanishi, K *et al.* (2008). Efficient adenovirus vector-mediated PPAR gene transfer into mouse embryoid bodies promotes adipocyte differentiation. *J Gene Med* **10**: 498–507.
27. Kubo, A, Chen, V, Kennedy, M, Zahradka, E, Daley, GQ and Keller, G (2005). The homeobox gene HEX regulates proliferation and differentiation of hemangioblasts and endothelial cells during ES cell differentiation. *Blood* **105**: 4590–4597.
28. Kovesdi, I, Brough, DE, Bruder, JT and Wickham, TJ (1997). Adenoviral vectors for gene transfer. *Curr Opin Biotechnol* **8**: 583–589.
29. Kawabata, K, Sakurai, F, Yamaguchi, T, Hayakawa, T and Mizuguchi, H (2005). Efficient gene transfer into mouse embryonic stem cells with adenovirus vectors. *Mol Ther* **12**: 547–554.
30. Koizumi, N, Mizuguchi, H, Utoguchi, N, Watanabe, Y and Hayakawa, T (2003). Generation of fiber-modified adenovirus vectors containing heterologous peptides in both the HI loop and C terminus of the fiber knob. *J Gene Med* **5**: 267–276.
31. Asahina, K, Fujimori, H, Shimizu-Saito, K, Kumashiro, Y, Okamura, K, Tanaka, Y *et al.* (2004). Expression of the liver-specific gene Cyp7a1 reveals hepatic differentiation in embryoid bodies derived from mouse embryonic stem cells. *Genes Cells* **9**: 1297–1308.
32. Moll, R, Franke, WW, Schiller, DL, Geiger, B and Krepler, R (1982). The catalog of human cytokeratins: patterns of expression in normal epithelia, tumors and cultured cells. *Cell* **31**: 11–24.
33. D'Amour, KA, Agulnick, AD, Eliazer, S, Kelly, OG, Kroon, E and Baetge, EE (2005). Efficient differentiation of human embryonic stem cells to definitive endoderm. *Nat Biotechnol* **23**: 1534–1541.
34. Touboul, T, Hannan, NR, Corbineau, S, Martinez, A, Martinet, C, Branchereau, S *et al.* (2010). Generation of functional hepatocytes from human embryonic stem cells under chemically defined conditions that recapitulate liver development. *Hepatology* **51**: 1754–1765.
35. Vallier, L, Touboul, T, Brown, S, Cho, C, Bilican, B, Alexander, M *et al.* (2009). Signaling pathways controlling pluripotency and early cell fate decisions of human induced pluripotent stem cells. *Stem Cells* **27**: 2655–2666.
36. Shiraki, N, Yoshida, T, Araki, K, Umezawa, A, Higuchi, Y, Goto, H *et al.* (2008). Guided differentiation of embryonic stem cells into Pdx1-expressing regional-specific definitive endoderm. *Stem Cells* **26**: 874–885.
37. Morrison, GM, Oikonomopoulou, I, Migueles, RP, Soneji, S, Livigni, A, Enver, T *et al.* (2008). Anterior definitive endoderm from ESCs reveals a role for FGF signaling. *Cell Stem Cell* **3**: 402–415.
38. Sumi, T, Tsuneyoshi, N, Nakatsuji, N and Suemori, H (2008). Defining early lineage specification of human embryonic stem cells by the orchestrated balance of canonical Wnt/beta-catenin, Activin/Nodal and BMP signaling. *Development* **135**: 2969–2979.
39. Xu, RH, Peck, RM, Li, DS, Feng, X, Ludwig, T and Thomson, JA (2005). Basic FGF and suppression of BMP signaling sustain undifferentiated proliferation of human ES cells. *Nat Methods* **2**: 185–190.
40. Keller, G (2005). Embryonic stem cell differentiation: emergence of a new era in biology and medicine. *Genes Dev* **19**: 1129–1155.
41. Selden, C, Shariat, A, McCloskey, P, Ryder, T, Roberts, E and Hodgson, H (1999). Three-dimensional *in vitro* cell culture leads to a marked upregulation of cell function in human hepatocyte cell lines–an important tool for the development of a bioartificial liver machine. *Ann N Y Acad Sci* **875**: 353–363.
42. Soto-Gutiérrez, A, Navarro-Alvarez, N, Zhao, D, Rivas-Carrillo, JD, Lebkowski, J, Tanaka, N *et al.* (2007). Differentiation of mouse embryonic stem cells to hepatocyte-like cells by co-culture with human liver nonparenchymal cell lines. *Nat Protoc* **2**: 347–356.
43. Kubo, A, Kim, YH, Irion, S, Kasuda, S, Takeuchi, M, Ohashi, K *et al.* (2010). The homeobox gene Hex regulates hepatocyte differentiation from embryonic stem cell-derived endoderm. *Hepatology* **51**: 633–641.
44. Hacein-Bey-Abina, S, Von Kalle, C, Schmidt, M, McCormack, MP, Wulffraat, N, Leboulch, P *et al.* (2003). LMO2-associated clonal T cell proliferation in two patients after gene therapy for SCID-X1. *Science* **302**: 415–419.
45. Sakamoto, N, Tsuji, K, Muul, LM, Lawler, AM, Petricoin, EF, Candotti, F *et al.* (2007). Bovine apolipoprotein B-100 is a dominant immunogen in therapeutic cell populations cultured in fetal calf serum in mice and humans. *Blood* **110**: 501–508.
46. Furue, MK, Na, J, Jackson, JP, Okamoto, T, Jones, M, Baker, D *et al.* (2008). Heparin promotes the growth of human embryonic stem cells in a defined serum-free medium. *Proc Natl Acad Sci USA* **105**: 13409–13414.
47. Mizuguchi, H and Kay, MA (1998). Efficient construction of a recombinant adenovirus vector by an improved *in vitro* ligation method. *Hum Gene Ther* **9**: 2577–2583.
48. Mizuguchi, H and Kay, MA (1999). A simple method for constructing E1- and E1/E4-deleted recombinant adenoviral vectors. *Hum Gene Ther* **10**: 2013–2017.
49. Maizel, JV Jr, White, DO and Scharff, MD (1968). The polypeptides of adenovirus. I. Evidence for multiple protein components in the virion and a comparison of types 2, 7A, and 12. *Virology* **36**: 115–125.
50. Suemori, H, Yasuchika, K, Hasegawa, K, Fujioka, T, Tsuneyoshi, N and Nakatsuji, N (2006). Efficient establishment of human embryonic stem cell lines and long-term maintenance with stable karyotype by enzymatic bulk passage. *Biochem Biophys Res Commun* **345**: 926–932.

TISSUE ENGINEERING: Part C
Volume 17, Number 2, 2011

DOI: 10.1089/ten.tec.2010.0139

Transplantation of Human Adipose Tissue-Derived Multilineage Progenitor Cells Reduces Serum Cholesterol in Hyperlipidemic Watanabe Rabbits

Hanayuki Okura, Ph.D.,[1,2] Ayami Saga, M.S.,[1] Yuichi Fumimoto, M.D., Ph.D.,[1] Mayumi Soeda, V.M.D.,[1] Mariko Moriyama, Ph.D.,[1,3] Hiroyuki Moriyama, Ph.D.,[3] Koji Nagai, M.D.,[1,4] Chun-Man Lee, M.D., Ph.D.,[1] Shizuya Yamashita, M.D., Ph.D.,[5] Akihiro Ichinose, M.D., Ph.D.,[4] Takao Hayakawa, Ph.D.,[3] and Akifumi Matsuyama, M.D., Ph.D.[1]

Familial hypercholesterolemia (FH) is an autosomal codominant disease characterized by high concentrations of proatherogenic lipoproteins and premature atherosclerosis secondary to low-density lipoprotein (LDL) receptor deficiency. We examined a novel cell therapy strategy for the treatment of FH in the Watanabe heritable hyperlipidemic (WHHL) rabbit, an animal model for homozygous FH. We delivered human adipose tissue-derived multilineage progenitor cells (hADMPCs) via portal vein and followed by immunosuppressive regimen to avoid xenogenic rejection. Transplantation of hADMPCs resulted in significant reductions in total cholesterol, and the reductions were observed within 4 weeks and maintained for 12 weeks. ^{125}I-LDL turnover study showed that the rate of LDL clearance was significantly higher in the WHHL rabbits with transplanted hADMPCs than those without transplanted. After transplantation hADMPCs were localized in the portal triad, subsequently integrated into the hepatic parenchyma. The integrated cells expressed human albumin, human alpha-1-antitrypsin, human Factor IX, human LDL receptors, and human bile salt export pump, indicating that the transplanted hADMPCs resided, survived, and showed hepatocytic differentiation *in vivo* and lowered serum cholesterol in the WHHL rabbits. These results suggested that hADMPC transplantation could correct the metabolic defects and be a novel therapy for inherited liver diseases.

Introduction

Familial hypercholesterolemia (FH) is characterized by premature and accelerated development of atherosclerotic lesions caused by elevated levels of cholesterol-rich lipoproteins in plasma. The disease is caused by mutations in the low-density lipoprotein (LDL) receptor gene that result in a significant decrease in receptor-mediated uptake of lipoproteins from the circulation.[1–3] Patients homozygous for defects in LDL receptors have serum cholesterol levels 5–10 times those of normal and suffer as early as the first two decades of life from complications such as coronary artery disease.[4,5] In homozygous FH patients, conventional drug therapy cannot treat the condition, and therapeutic recourses are limited to chronic plasmapheresis or orthotopic liver transplantation.[1] Although liver transplants lower LDL levels, the procedure is life threatening; in addition, donor livers are in short supply. Cellular transplantation has been proposed to provide functional LDL receptors for the treatment of hypercholesterolemia. Transplantation of allogenic and xenogenic hepatocytes has been shown to be effective in lowering serum cholesterol in the Watanabe heritable hyperlipidemic (WHHL) rabbit,[6–9] which is an animal model for homozygous FH. Further, a number of gene therapy approaches have shown some promises in animal models and human,[10–13] and the therapies will cure a number of patients with FH in near future. As an alternative to whole-organ transplantation and/or gene therapy, we have investigated the ability of human adipose tissue-derived multilineage progenitor cells (hADMPCs) to differentiate into hepatocytes *in vitro* and to replace critical liver functions[14] as well as previous reports,[15,16] because the *in vitro* differentiation of hADMPCs into various kinds of cell types in now well reported and hADMPCs can be easily and safely obtained in large

[1]Department of Somatic Stem Cell Therapy and Health Policy, Foundation for Biomedical Research and Innovation, Kobe, Japan.
[2]Research Fellow of the Japan Society for the Promotion of Science, Tokyo, Japan.
[3]Pharmaceutical Research and Technology Institute, Kinki University, Osaka, Japan.
[4]Department of Plastic Surgery, Kobe University Hospital, Kobe, Japan.
[5]Division of Cardiology, Department of Internal Medicine, Osaka University Graduate School of Medicine, Osaka Japan.

quantities without serious ethics issues.[17,18] In this study, we are investigating whether hADMPCs could differentiate into hepatocytes *in vivo* and replace critical liver functions as considerable therapeutic potential for cellular replacement.

Materials and Methods

Cells

hADMPCs were prepared as described previously[19] with some modifications.[14,17,18] Adipose tissues from human subjects were resected during plastic surgery in five subjects (four males and one female, age, 20–60 years) as excess discards. Ten to 50 g of subcutaneous adipose tissue was collected from each subject. All subjects provided informed consent. The protocol was approved by the Review Board for Human Research of Kobe University Graduate School of Medicine, Osaka University Graduate School of Medicine, and Foundation for Biomedical Research and Innovation. After five to six passages, the hADMPCs were used for transplantation. Human cryopreserved hepatocytes were purchased from Invitrogen (Lot number: HuP81) and cultured as indicated by the manufacturer's protocol. Human adipose tissue-derived fibroblastic cells were obtained according to previous report.[20]

Flow cytometric analysis

hADMPCs isolated from adipose tissue were characterized by flow cytometry. Cells were detached from culture dishes by 0.25% trypsin/ethylenediaminetetraacetic acid (EDTA) and suspended in Dulbecco's phosphate-buffered saline (DPBS; Nacalai Tesque) containing 0.1% fetal bovine serum. Aliquots (5×10^5 cells) were incubated for 30 min at 4°C with fluorescein isothiocyanate-conjugated mouse monoclonal antibodies to human CD31 (BD PharMingen), CD105 (Ancell Corporation), CD133 (R&D Systems), phycoerythrin-conjugated mouse monoclonal antibodies to human CD29, CD34, CD45, CD73 (BD PharMingen), CD44, or CD166 (Ancell). Isotype-identical antibodies served as controls. Further, the cells were incubated with mouse monoclonal antibodies against human stage-specific embryonic antigen-4 (from Chemicon International, Inc.), ABCG-2, or CD117 (BD PharMingen) with nonspecific mouse antibody used as a negative control. After washing with DPBS, cells were incubated with phycoerythrin-labeled goat anti-mouse Ig antibody (BD PharMingen) for 30 min at 4°C. After three washes, cells were resuspended in DPBS and analyzed by flow cytometry using a FACSCalibur flow cytometer and CellQuest Pro software (BD Biosciences).

Adipogenic, osteogenic, and chondrogenic differentiation procedure

For adipogenic differentiation, cells were cultured in the differentiation medium (Zen-Bio, Inc.). After 3 days, half of the medium was changed with adipocyte medium (Zen-Bio) every 2 days. Five days after differentiation, adipocytes were characterized by microscopic observation of intracellular lipid droplets by Oil Red O staining. Osteogenic differentiation was induced by culturing the cells in Dulbecco's modified Eagle's medium containing 10 nM dexamethasone, 50 mg/dL ascorbic acid 2-phosphate, 10 mM β-glycerophosphate (Sigma), and 10% fetal bovine serum. Differentiation was examined by Alizarin red staining. For Alizarin red staining, the cells were washed three times and fixed with dehydrated ethanol. After fixation, the cells were stained with 1% Alizarin red S in 0.1% NH_4OH (pH 6.5) for 5 min and then washed with H_2O. For chondrogenic differentiation, hADMPCs were first trypsinized and 2×10^5 cells were centrifuged at 400 *g* for 10 min. The resulting pellets were cultured in the chondrogenic medium (alpha-minimum essential medium (alpha-MEM) supplemented with 10 ng/mL transforming growth factor-β, 10 nM dexamethasone, 100 μM ascorbate, and 10 μL/mL 100×ITS Solution) for 14 days. For Alcian Blue staining, nuclear counterstaining with Weigert's hematoxylin was followed by 0.5% Alcian Blue 8GX for proteoglycan-rich cartilage matrix.

hADMPC transplantation and immunosuppression regimen

WHHL rabbits (8 weeks old; purchased from Kitayama-labes, Inc.) were anesthetized with pentobarbital (50 mg/kg). An incision distal and parallel to the lower end of the ribcage was made. The peritoneum was incised, and hADMPCs ($n=5$) or human adipose tissue-derived fibroblastic cells ($n=3$) (3×10^7 cells) suspended in 3 mL of Hanks' balanced salt solutions (HBSS) (20°C) or 3 mL of control saline ($n=6$) were infused in 5 min into the portal vein via a 18-gauge Angiocath™ (BD). The immunosuppression regimen (Fig. 1A) consisted of the following: (1) intramuscular injection of cyclosporin A (6 mg/kg/day) daily from the day before surgery to sacrifice; (2) intramuscular injection of rapamycin (0.05 mg/kg/day) daily from the day before surgery to sacrifice; (3) methylprednisolone at 3 mg/kg/day (days 1–7), followed by tapering to 2 mg/kg/day (days 8–14), 1 mg/kg/day (days 15–21) and 0.5 mg/kg/day (day 22 to the time at sacrifice); (4) intravenous injection of cyclophosphamide (20 mg/kg/day) at days 0, 2, 5, and 7; (5) ganciclovir (2.5 mg/kg/day intramuscular injection (i.m.)) was also administrated to avoid viral infection in the immunocompromised host.

DNA extraction and quantification of human-derived cells

Total DNA of WHHL rabbit liver, which was obtained at the time just after hADMPC transplantation, and 2, 4, 8, and 12 weeks after transplantation, were isolated using a NucleoSpin Tissue kit (Macherey-Nagel) according to the manufacturer's instructions. hADMPCs and rabbit hepatocytes were mixed at the ratios of 100:0 (100%), 10:90 (10%), 1:99 (1%), 0.1:99.9 (0.1%), 0.01:99.99 (0.01%), and 0.001:99.999 (0.001%), and DNA was isolated. Seven hundred nanograms of each samples of extracted DNA was quantified by real-time polymerase chain reaction (PCR) using the ABI Prism 7900 Sequence Detection System (Applied Biosystems), primers for the 82 bp *Alu* amplicon (forward, 5′-GTCAGGAGATCGA GACCATCCC; reverse, 5′-CCACTACGCCCGGCTAATTT), and SYBR Green (TOYOBO) dye using a previously published protocol.[21,22] Reactions were performed in quadruplicate and the *Alu* levels were calculated by the standard curve.

Assay for lipid profiling

Serum samples were obtained from nonfasting rabbits before and after transplantation. Serum total cholesterol was measured in each sample using assay kits from Wako Pure Chemical Industries. Serum lipoproteins were analyzed by an on-line dual enzymatic method for simultaneous quantification of cholesterol and triglycerides by high-performance